



CATALYTIC PARTIAL OXIDATION REFORMING OF JP8 AND S8

THESIS

Thomas G. Howell

AFIT/GAE/ENY/07-J08

**DEPARTMENT OF THE AIR FORCE
AIR UNIVERSITY**

AIR FORCE INSTITUTE OF TECHNOLOGY

Wright-Patterson Air Force Base, Ohio

APPROVED FOR PUBLIC RELEASE; DISTRIBUTION UNLIMITED

The views expressed in this thesis are those of the author and do not reflect the official policy or position of the United States Air Force, Department of Defense, or the U.S. Government.

AFIT/GAE/ENY/07-J08

CATALYTIC PARTIAL OXIDATION REFORMING OF JP8 AND S8

THESIS

Presented to the Faculty

Department of Aeronautics & Astronautics

Graduate School of Engineering and Management

Air Force Institute of Technology

Air University

Air Education and Training Command

In Partial Fulfillment of the Requirements for the
Degree of Master of Science in Aeronautical Engineering

Thomas G. Howell, B.S.

June 2007

APPROVED FOR PUBLIC RELEASE; DISTRIBUTION UNLIMITED

CATALYTIC PARTIAL OXIDATION REFORMING OF JP8 AND S8

Thomas G. Howell, B.S.

Approved:

Richard Branam, Maj, USAF (Chairman)

Date

Joerg Walter, Maj, USAF (Member)

Date

Jonathan Black, PhD (Member)

Date

Thomas Reitz, PhD (Member)

Date

Abstract

Catalytic partial oxidation (CPOX) reforming experiments were performed using a 10 kW Aspen Products Group, Inc. fuel processing prototype utilizing military logistic fuels JP8 and S8. S8 is a sulfur-free Fisher-Tropsch fuel, while JP8 is a multi-fuel blend, which could impact reforming efficiency, product distribution and byproduct production. Sulfur contained within the JP8 will adversely affect the product distribution; therefore, desulfurization beds, capable of removing up to 1000 ppm sulfur, were incorporated into the system. The catalyst used in the prototype is noble metal dispersed on cordierite monolith. The goal of this experiment was to evaluate the efficiency and product distribution of the prototype fuel processor through application of several potential military fuels. These results are compared with computational models (Stanjan) to determine if CPOX reactions can be appropriately modeled. JP8 with 700 ppm of sulfur had the highest efficiency of 84.62% followed by JP8 with 400 ppm of sulfur at 84.37% and S8 at 84.37%.

Acknowledgments

I would like to thank my faculty advisor, Major Branam, for his guidance and support throughout my thesis work. The insight and experience was certainly appreciated and his willingness to take on additional thesis students was admirable. I would, also, like to thank my sponsor, Dr. Thomas Reitz, from the Air Force Research Labs for the support and knowledge that he provided to me. Dr. Thomas Reitz provided me with the proper guidance and genuine interest in the experiment to make this thesis an enjoyable experience. I would like to thank my thesis committee members, Dr. Black and Major Walter, for taking the time out of their schedules. Thanks to Tom Jenkins, Tom Greene, Michael Rottmayer, and Mark Fokema for their assistance with my project. I would like to show my appreciation for my parents and family who always encouraged me to continue my education. I would like to recognize my girlfriend who has motivated me and helped me during my graduate school career.

Thomas G. Howell

AFIT/GAE/ENY/07-J08

*In memory of
Grandma and Grandpa*

Table of Contents

	Page
Abstract.....	iv
Acknowledgments.....	v
Dedication.....	vi
Table of Contents.....	vii
List of Figures.....	ix
List of Tables.....	xii
I. Introduction.....	1
Background.....	1
Research Objectives.....	4
II. Literature Review.....	5
Chapter Overview.....	5
Types of Fuel Cells.....	5
Fuel Reforming: Internal or External.....	13
Fuels Used in Fuel Reforming.....	13
Variation in Methods of Fuel Reforming.....	14
III. Methodology.....	20
Aspen Fuel Processor.....	20
Error Estimates.....	25
IV. Analysis and Results.....	29
Results from Stanjan Simulations.....	29
Results from Aspen Reformer.....	42

V. Conclusions and Recommendations	55
Conclusions of Research	55
Significance of Research	56
Recommendations for Future Research.....	56
Appendix.....	60
Bibliography	65
Vita.....	68

List of Figures

	Page
Figure 1: How solid oxide fuel cells work (US Department of Energy, 2007)	7
Figure 2: How molten carbonate fuel cells work (US Department of Energy, 2007)	8
Figure 3: How polymer electrolyte membrane fuel cell work (US Department of Energy, 2007)	9
Figure 4: How phosphoric acid fuel cells work (US Department of Energy, 2007)	11
Figure 5: How alkaline fuel cells work (US Department of Energy, 2007)	12
Figure 6: Hydrogen varying O/C ratio with statistical error.....	27
Figure 7: Hydrogen varying O/C ratios showing O/C ratio systematic uncertainty.....	28
Figure 8: The effects of aromatics on hydrogen selectivity with respect to temperature .	30
Figure 9: The effects of aromatic on coking with respect to temperature	31
Figure 10: Effect of varying O/C ratio on the production of hydrogen with respect to temperature.....	32
Figure 11: The effects of varying O/C ratios on coking with respect to temperature	33
Figure 12: Major carbon products with an O/C ratio of 1.04 with respect to temperature	34
Figure 13: Major hydrogen products with an O/C ratio of 1.04 with respect to temperature.....	35
Figure 14: Carbon selectivity to methane with varying O/C ratios with respect to temperature.....	36
Figure 15: Hydrogen selectivity to water varying O/C ratios with respect to temperature	37

Figure 16: Carbon selectivity to carbon dioxide with varying O/C ratio with respect to temperature.....	38
Figure 17: Carbon selectivity to carbon monoxide with varying O/C ratios with respect to temperature.....	39
Figure 18: Carbon selectivity to ethylene with varying O/C ratios with respect to temperature.....	40
Figure 19: Sulfur selectivity for the major sulfur products at 31% aromatics and O/C ratio of 1.04 with respect to temperature.....	41
Figure 20: The effects of sulfur content in fuels on the production of hydrogen	46
Figure 21: Constant hydrogen production over a long period of time with fuels of various sulfur levels	47
Figure 22: The effects of varying O/C ratios on the production of hydrogen with various fuels and modeled fuels.....	48
Figure 23: The effects of varying O/C ratios on the CO production with various fuels and modeled fuels	49
Figure 24: The effects of varying O/C ratios on the CO ₂ production with various fuels and modeled fuels	50
Figure 25: Predicted efficiency for the Aspen reformer using JP8 or S8 with respect to O/C ratios	51
Figure 26: Efficiency of Aspen Reformer with various fuels and modeled fuels with respect to O/C ratios.....	52

Figure 27: Projected efficiency values for the Aspen reformer with varying O/C ratios for various fuels	53
Figure 28: CPOX reforming of JP8 with varying O/C ratios with respect to temperature	57
Figure 29: Steam reforming of JP8 with varying steam to carbon ratios with respect to temperature.....	58
Figure 30: Auto-thermal reforming with JP8 varying steam to carbon ratios with respect to temperature.....	59
Figure 31: CO varying O/C ratio with statistical error	61
Figure 32: CO varying O/C ratios showing O/C ratio systematic error	62
Figure 33: CO ₂ varying O/C ratios with statistical error	63
Figure 34: CO ₂ varying O/C ratios showing O/C ratio systematic error	64

List of Tables

Table 1: Standard deviation of reformat mole fraction values.....	26
Table 2: Percent error of mole fraction reformat values	27
Table 3: Stanjan predictions for design point using JP8.....	42
Table 4: Heats of Combustion for fuels and reformat.....	44
Table 5: Design points for Aspen reformer with varying fuels	54
Table 6: Sample calculation for GC data on JP8 with 700 ppm sulfur.....	60
Table 7: Sample calculation for mass balance on JP8 with 700 ppm sulfur.....	60
Table 8: Sample calculations for Efficiency and Power on JP8 with 700 ppm sulfur.....	60

CATALYTIC PARTIAL OXIDATION REFORMING OF JP8 AND S8

I. Introduction

Background

William Grove developed the first hydrogen fuel cell in 1839. In Grove's experiment, water was electrolyzed into hydrogen and oxygen by providing a small current through it. (Larminie et al, 2000) This initial experiment shed some light as to how making the electrodes flat and porous, to allow both gas and electrolyte to pass through, increases the current provided by the fuel cell. Ensuring the electrodes are flat and porous results in maximum contact between the electrode, electrolyte and the gas.

Fuel cells take chemical energy from fuel and convert it into electricity. These cells require hydrogen supplied to an anode and oxygen to a cathode. Between the anode and cathode is an ion-conducting electrolyte material. The anode serves as the negatively charged electrode while the cathode is the positively charged electrode. The electrons must go through the electrolyte material to reach the oppositely charged site, providing an exploitable electric load. (Song 2002) A big advantage of fuel cells is the lack of moving parts and the fact they are more efficient at providing electricity versus internal combustion engines. Fuel cells have the ability to not only reduce harmful nitrous oxides (NO_x) emissions but also to increase the efficiency of fuel based power generation by a factor of two. (Song 2002) The major challenge in fuel cells is creating a constant hydrogen rich stream needed as fuel for the cells.

A reforming process is necessary since hydrogen storage tanks present safety issues. The current need for a hydrogen rich fuel stream for fuel cells has driven the desire to convert military fuels, such as JP8, to hydrogen. Reforming of fuels such as JP8 using catalytic partial oxidation (CPOX) can provide many advantages over internal combustion engines by reducing the carbon dioxide (CO₂) emissions, lowering the noise signature and making the system more energy efficient. CPOX reduces CO₂ emissions by creating more carbon monoxide (CO) used in fuel cells. CO is valuable for system efficiency due to the heat of combustion value for CO. By reforming JP8 to produce hydrogen, fuels burn more efficiently and emissions are reduced. The current internal combustion engines are only 20% to 35% efficient while fuel cell systems could have an efficiency of 40% to 50% (Song 2002). Reforming JP8 versus a fuel like methane is beneficial since the conversion for JP8 is above 99%. Conversion of methane is around 85% to 95% (Krummenacher et al. 2003).

The hydrogen rich stream of fuel created when hydrocarbon fuels are reformed can be used in different ways with different fuel cells. For example, polymer electrolyte membrane fuel cells can function on reformed pretreated hydrocarbons fuels, or on hydrogen (H₂). Hydrogen fuel can be used for polymer electrolyte membrane fuel cells, which could be used to power vehicles. These fuel cell vehicles would have a system on-board converting gasoline to hydrogen and CO. For a vehicle powered by fuel cells, the fuel will need to be low in sulfur and aromatics in order to prevent the sulfur from poisoning the catalyst. With the current fuel efficiency of cars of about 12% to 15%,

there is much room for improvement and a fuel cell powered car can be two to three times more efficient than existing vehicles. (Song 2002)

Molten carbonate fuel cells can use the hydrogen stream created from reforming hydrocarbons. A molten carbonate fuel cell is a high temperature fuel cell operating around 50% to 60% efficiency. The heat used by the fuel cell could be used to generate more electricity in a combined cycle system. Molten carbonate fuel cells are ideally suited for a stationary electric power plant due to the problems of cracking when heating or cooling the system. (Song 2002)

Phosphoric acid fuel cell systems have demonstrated the capability of running on reformed hydrocarbon fuels. Phosphoric acid fuel cell systems can have a fuel to electricity efficiency of 40% to 45%. Phosphoric acid fuel cells are the most developed fuel cell technology and already boast more than seventy plant sites in the United States, Japan and Europe. By providing hydrogen streams to different fuel cells, stationary or mobile power plants can achieve an increase in efficiency. The internal combustion engine can benefit from using reformed hydrocarbons for fuel cell vehicles by improving the efficiency by two or three times, while decreasing the emissions produced. With on-board fuel reforming for fuel cell cars, there would be no change to the current infrastructure of existing gasoline stations. (Song 2002)

Research Objectives

The desired outcome of this investigation is a device producing a steady and constant stream of hydrogen fuel through reforming. The goal is then to experimentally investigate JP8 and S8 performance with catalytic partial oxidation reforming to show the effects of sulfur and different aromatic components in fuel on the reforming process. Predictions suggest S8 should produce more hydrogen since it does not contain any sulfur, which poisons the catalyst. Coking should be reduced for this fuel as well due to fewer aromatics. This research will focus on catalytic partial oxidation reforming of two different fuels, JP8 and S8, containing varying sulfur content and percentages of aromatics.

II. Literature Review

Chapter Overview

This chapter discusses different types of fuel cells, fuels used in fuel reforming and different types of fuel reforming. The goal of this chapter is to make the reader familiar with past and present fuel cells and fuel reforming technologies.

Types of Fuel Cells

A problem some fuel cells have is a slow reaction rate. Researchers have addressed this problem in three ways. One solution is the use of a catalyst to speed up the reaction rates. A second method for increasing reaction rates is to raise the temperature of the fuel cell. The third technique is to increase the surface area of the electrode. (Larminie et al, 2000)

The corrosive nature of some fuels and coking directly affects the surface area of the electrode. The main issues concerning the use of fuel cells are hydrogen is the most commonly used fuel and the reaction rates can be slow, leading to low current and power output.

Many different types of fuel cells address the issues of coking, sulfur poisoning, and slow reaction rates. The five major types of fuel cells are solid oxide fuel cells (SOFC), molten carbonate fuel cells (MCFC), polymer electrolyte membrane fuel cells (PEMFC), phosphoric acid fuel cells (PAFC) and alkaline fuel cells (AFC). These fuel cells can use two types of metals as catalysts. They can have either precious metal or non-precious metal catalysts. The typical non-precious metal catalyst is nickel (Ni), which is supported on aluminum oxide (Al_2O_3). The non-precious metal catalysts are

normally found in MCFC and SOFC. The most common precious metal catalyst is platinum (Pt) and is also supported on Al_2O_3 . The precious metal catalyst can be found in PEMFC and PAFC. (Larminie et al, 2000)

In addition, fuel cells can be separated into the categories of high and low temperature fuel cells. The high temperature fuel cells are SOFC and MCFC, while low temperature fuel cells are AFC, PEMFC and PAFC. (Larminie et al, 2000)

SOFC contain an oxide ion conducting ceramic electrolyte, beneficial since it will prevent corrosion. The electrolyte material, yttria stabilized on zirconia (YSZ) is highly stable in oxidizing and reducing environments. SOFC are similar to MCFC, both using hydrogen and carbon monoxide as fuel. SOFC uses a negatively charged ion transferring from the cathode through the electrolyte to the anode, similar to MCFC types. (Larminie et al, 2000) SOFC are high temperature fuel cells normally operating at a temperature range of 650°C to 1100°C (Song 2002). The commonly used electrolyte for SOFC is zirconia (ZrO) with a small amount (6% to 10%) of yttria (Y_2O_3) as a stabilizer. The reason SOFC must be a high temperature fuel cell is at approximately 800°C , YSZ becomes a conductor for negatively charged oxygen ions. (Larminie et al, 2000) The typical anode for a SOFC is composed of zirconia with nickel as the metallic component. Nickel provides high electric conductivity for the anode. The cathode material has varied because of the cost of noble metals. (Larminie et al, 2000)

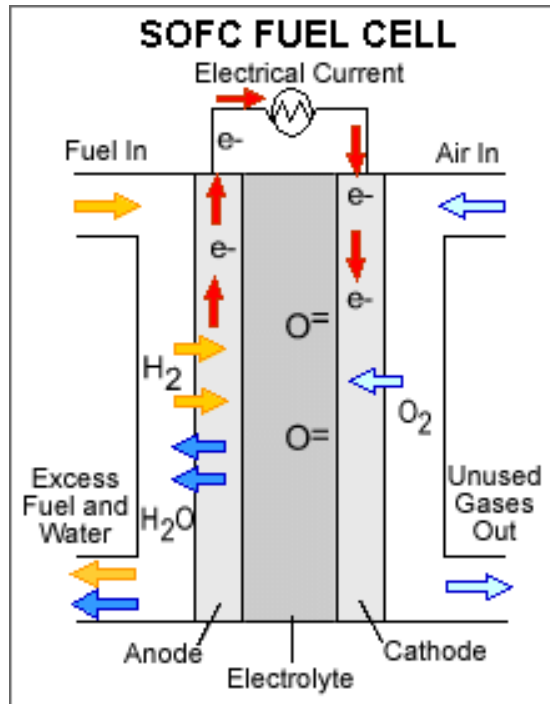


Figure 1: How solid oxide fuel cells work (US Department of Energy, 2007)

SOFC are a good choice for on-board reforming of fuels due to the high fuel cell operating temperatures (650°C to 1100°C). With the high operating temperature the excess heat could be used in thermal electricity generating plants, increasing the fuel efficiency. Due to the high operating temperature, there is a significant start-up time required for SOFC. These fuel cells are fairly sensitive to operating temperature. For example, performance decreases of about 12% have been realized if the temperature drops to 900°C from 1100°C. Due to the high temperatures involved, these devices require a large amount of thermal shielding, making it harder to create small and portable SOFC. (Song 2002)

MCFC initially operated with coal as the fuel. Today, researchers endeavor to use MCFC with natural gas as a fuel. MCFC have a carbonate electrolyte supported on a

lithium aluminum oxide (LiAlO). The anode is a Ni-Cr/Ni-Al alloy, while the cathode is nickel oxide (NiO). The difference between MCFC and other fuel cells is MCFC have the components stacked together and are heated to operating temperature over a period of approximately 14 hours. Having the components stacked together and heated causes expansion and contraction. If heating and cooling are not done slowly, the electrolyte will crack causing a direct connection from the anode to cathode. (Larminie et al, 2000)

The fuel cell normally operates at a temperature of 650°C. MCFC are temperature sensitive as well. A drop in temperature of 50°C could cause a drop in voltage of approximately 15%. The downfall to an MCFC is the cathode needs a source of CO₂ in order to create a carbonate ion. (Song 2002)

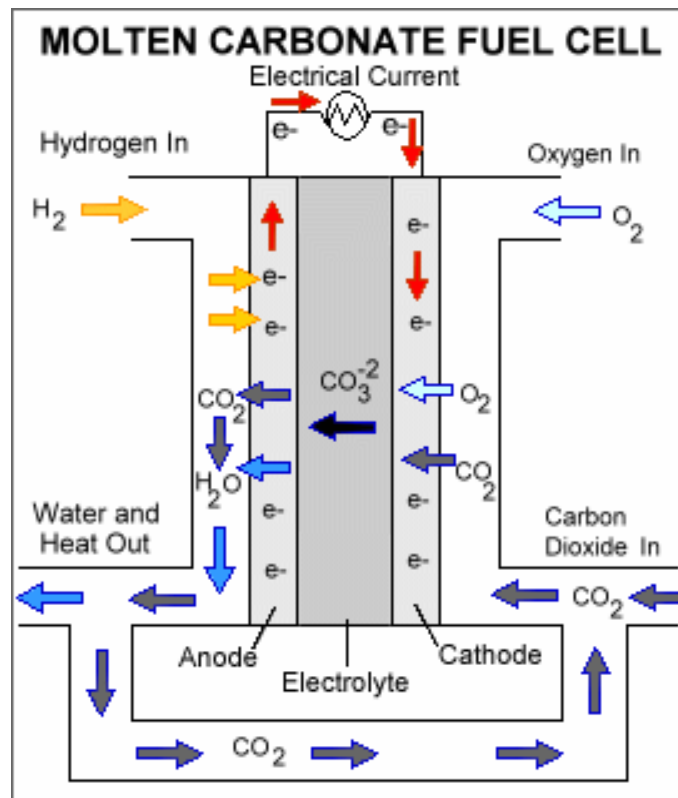


Figure 2: How molten carbonate fuel cells work (US Department of Energy, 2007)

PEMFC have membrane electrode assemblies (MEA); the anode, electrolyte and cathode are assembled as one. PEMFC are compact fuel cells due to the thinness of the MEA. The anode and cathode for normal PEMFC are platinum (Pt) based. The electrolyte for a PEMFC is typically polytetrafluoroethylene (PTFE). The strong bonds between carbon and fluorine allow for the electrolyte to be tough and able to withstand chemical attacks. PTFE is hydrophobic driving the water away from the electrodes, therefore water management is a major issue in PEMFC. (Larminie et al, 2000)

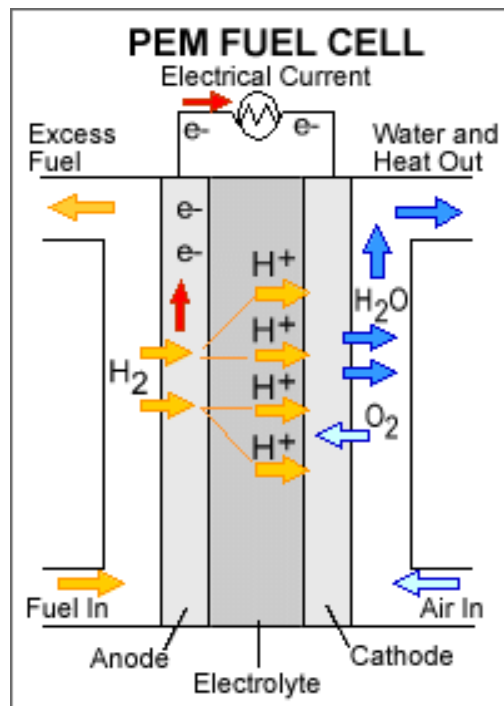


Figure 3: How polymer electrolyte membrane fuel cell work (US Department of Energy, 2007)

The one problem with PEMFC is that CO will poison the Pt based anode. CO is a product of reforming fuel. One method to reduce the CO poisoning is to use a Pt-Ru anode catalyst (Paulus et al. 2000). Even with a Pt-Ru anode catalyst, the fuel for a

PEMFC must contain less than 30 ppm of CO in order for the catalyst to function properly. The three ways CO can be reduced are methanation, membrane separation and selective oxidation. Methanation converts CO and H₂ using hydrogenation to create methane, which will not poison the catalyst. The downfall of methanation is it removes hydrogen that could otherwise be used as fuel for fuel cells, to make the methane. Membrane separation removes hydrogen separated from the gas mixtures. The membrane used is normally palladium. This membrane allows the hydrogen created to be used as fuel in the fuel cell. This process uses selective oxidation by incorporating a small amount of air into the gas stream. This resulting stream then passes over a precious metal catalyst where CO is absorbed. The normal operating temperature of a PEMFC is between 70°C and 90°C allowing for immediate start up at 50% power and full power in about three minutes. Since PEMFC operational temperatures are so low, they do not provide heat for the reforming process of hydrocarbons. The biggest problem with PEMFC is the membrane needs to be hydrated. Therefore, the cell needs to operate at temperatures (70°C to 90°C) to prevent the water from evaporating quickly. The biggest benefit is the order of magnitude higher power density compared to any other fuel cell (except for AFC, which will have a similar power density). With the high power density, PEMFC offers a reduction in size and cost. The low operational temperature requires PEMFC to have little or no thermal shielding. (Song 2002) By having lower operational temperatures this provides less heat rejection. This heat rejected by the fuel cell can be used in steam reforming as an external heat source.

PAFC has a phosphoric acid (H_3PO_4) electrolyte, beneficial since it is tolerant to carbon monoxide. A disadvantage of using phosphoric acid is the relatively high freezing point (42°C). With this high freezing point, the electrolyte must be kept above 42°C to prevent mechanical stress on the stack due to freezing and thawing of the electrolyte. Similar to PEMFC, the anode and cathode of PAFC are platinum based. The stack for a PAFC contains ribbed bipolar plates serving as dividers for the individual cells, while connecting them in series and providing the fuel to the anode and cathode. (Larminie et al, 2000)

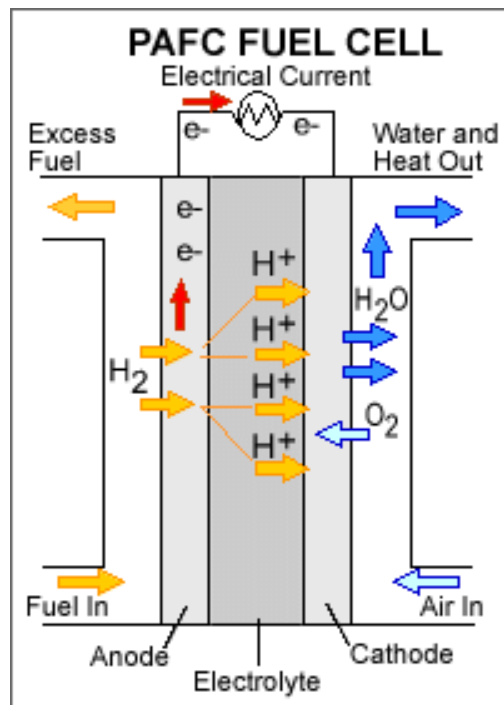


Figure 4: How phosphoric acid fuel cells work (US Department of Energy, 2007)

PAFC has the advantage of easy water management over PEMFC since it uses concentrated acid, thereby reducing the water vapor pressure. PAFC systems normally have an operating temperature of 180°C to 220°C . The problem with PAFC is CO

poisoning the catalyst. A water-gas shift reaction is necessary to reduce CO and prevent the reduced catalyst capability. (Song 2002)

AFC are phasing out due to some major downfalls; they require pure H_2 and are sensitive to CO_2 . AFC has a water problem similar to PEMFC except the cell produces water at the anode and removes it at the cathode. AFC did have the benefit of being simple to design with an inexpensive electrolyte, potassium hydroxide (KOH). Added to this benefit, the AFC reduces oxygen through a quick process and in turn allows for higher operating voltages. AFC do not use bipolar plates and have non-precious metal for the anode and cathode, also contributing to the lower cost for AFC. (Larminie et al, 2000)

The operating temperature for AFC can vary from $120^\circ C$ to $250^\circ C$ based on the concentration of KOH (Song 2002).

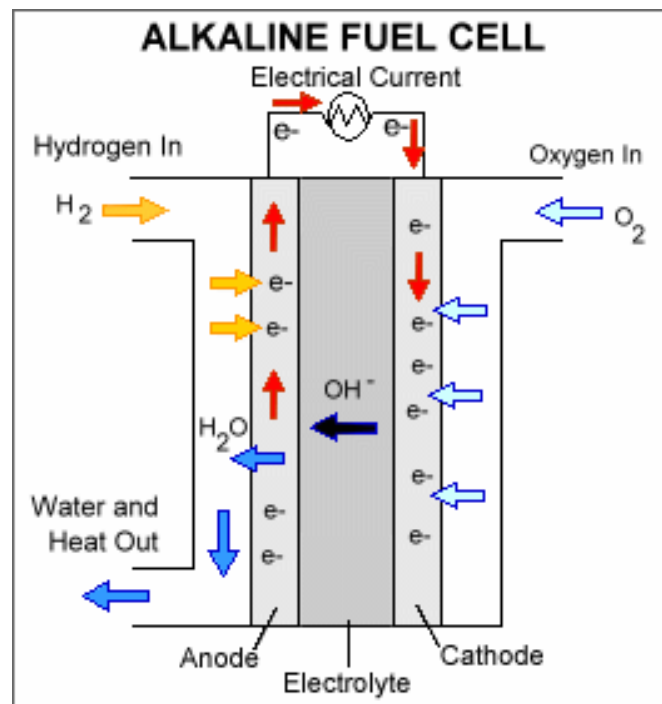


Figure 5: How alkaline fuel cells work (US Department of Energy, 2007)

Fuel Reforming: Internal or External

There are two ways to implement fuel reforming: internal and external reforming. External reforming is a reforming process using steam reforming, catalytic partial oxidation or auto-thermal reforming. For internal reforming, two different methods may be used. The first is direct internal reforming where both fuel reforming and an electrochemical reaction occur in the same anode chamber. With indirect internal reforming, the fuel reforming and the electrochemical reaction occur on opposite sides of the anode chamber.

Advantages of using internal reforming over external reforming include the reduction in space required and an increase in efficiency of the system. The current internal combustion engines are only 20% to 35% efficient while fuel cell systems have an efficiency of 40% to 50% (Song 2002). This would help lower the energy demand placed on the ever-decreasing energy supplies.

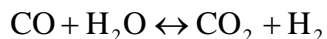
Fuels Used in Fuel Reforming

In fuel reforming, alcohol or hydrocarbons are used as the fuels. Alcohol fuels are favorable since they are sulfur free and can reform at low temperatures. However, hydrocarbon fuels are preferred due to their higher energy densities. Hydrocarbon fuels require a system to remove the sulfur and prevent coking. A current method used to reduce the sulfur content in fuel is selective absorption, with a mixture of nickel and nickel monoxide at 150°C. In an experiment by Lenz et al, sulfur content was reduced in Jet A-1 from 290 ppmw to 1.2 ppmw. (Lenz et al., 2005) Fuels such as JP8 are heavy hydrocarbons potentially leading to large amounts of carbon deposits forming. Also,

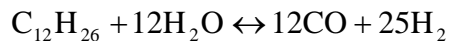
fuels having a large amount of aromatics lead to even more carbon formation. With a fuel such as JP8, the goal is to reform the fuel into small molecules (i.e. H₂). Smaller fuel molecules burn more efficiently and decrease the emissions produced.

Variation in Methods of Fuel Reforming

Fuel reforming can use one of three different methods. Steam reforming is an endothermic reaction producing CO and H₂ when adding hydrocarbon fuel and water. Some fuel cells, such as PEMFC, have a catalyst that can be easily poisoned by CO. Therefore, they can undergo a water-gas shift to produce CO₂ and H₂ as shown below.



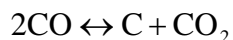
Steam reforming is used in industry for large-scale hydrogen production (Larminine et al. 2000). An example of steam reforming is:



Steam reforming also has the problem of coking from dehydrogenation and CO disproportion (Boudouard reaction) leading to deactivation of the catalyst. To reduce the effects of coking, researchers have used a high steam to carbon ratio or a carbon resistant catalyst such as a noble metal. An example of dehydrogenation is:



Dehydrogenation is an undesirable result since it leads to a large amount of carbon being produced, thereby causing coking and deactivating the catalyst. An example of a Boudouard reaction is:

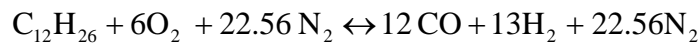


The computational model described later shows this reaction (Hardiman et al. 2004).

A study of thermal efficiency of steam reforming heptane at 800°C using two kinetic computer modeling tools (Chemkin and Stanjan) illustrates the best results occur at a steam to carbon ratio of 2.25 (Lutz et al. 2004). With the lower steam to carbon ratios, a small amount of methane is present in the system, decreasing the amount of hydrogen available. This study also showed the maximum hydrogen production occurs at approximately 600°C. This maximum indicates the point of zero methane. If the temperature is increased above 600°C, hydrogen production will decrease due to the water-gas shift increasing the production of CO. (Lutz et al. 2004) Steam reforming is a common practice today to produce hydrogen using light hydrocarbons such as methane (CH₄). With steam reformation, an increase in pressure will cause the reaction to increase the amount of CH₄ produced and a reduction in pressure will increase the amount of H₂ produced based on LeChatelier's principle. Using LeChatelier's principle, an increase in temperature would cause the amount of hydrogen produced to increase. (Larminine et al. 2000) The current commercial catalysts used are Ni based with a support such as calcium monoaluminate (CaAl₂O₄) or magnesium oxide (MgO) and have temperatures above 500°C. A kinetics study of steam reformation of isooctane has been performed. Temperatures at the end of the catalyst bed below 523 K (249.85° C) would result in unacceptable reactions (Praharso et al. 2004). The problem with larger hydrocarbons is coking; therefore, precious metal catalysts are needed to reduce the coking. Using ceria as a support increases the activity, and has proven to be better than the alumina supported catalysts (Wang et al. 2002). For steam reforming, larger hydrocarbons need a larger H₂O/C ratio to have a stable reaction (Wang et al. 2002). The

ceria support does not resist carbon deposits decreasing the reaction rates (Wang et al. 2002). In a study using cerium (Ce) on a nickel/zeolite (Ni/ZSM-5) catalyst, the acid sites provided from the Ce will increase the cracking of the hydrocarbon while also increasing the oxidative steam reforming reaction. In this same study, the addition of magnesium (Mg) caused the activity of the catalyst to decrease. (Wang et al. 2005) Cobalt-nickel (Co-Ni) catalysts increase the temperature and the steam to carbon ratio decreasing carbon build up on the catalysts (Hardiman et al. 2004). But increasing the steam to carbon ratio decreases the efficiency of the system because more heat is required. By having a partial oxidation reaction, the amount of hydrogen produced is greatly increased. (Wang et al. 2005) This is the idea behind auto-thermal reforming discussed later.

The second method of fuel reforming is a catalytic partial oxidation (CPOX) reaction resulting in H₂ and CO production. An example of a CPOX reaction is:

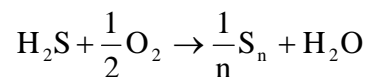


The reaction above is at oxygen (O) to carbon (C) ratios of 1.0, with only CO, H₂ and nitrogen (N₂) as products, theoretically. Comparing the steam reforming to CPOX reforming, one molecule of dodecane will produce 25 H₂ molecules using steam reforming while the CPOX reaction will produce 13 H₂ molecules. Steam produces more hydrogen per molecule of fuel but CPOX reforming is exothermic. Therefore, it is different than steam reforming since no external heat source is required. Steam reforming can use the heat rejected from the fuel cells as the external heat source. Some disadvantages of catalytic partial oxidation are coking and overheating because it is an exothermic process.

Partial oxidation has been looked at previously but the benefits in hydrogen production with a catalyst have led to the investigation of CPOX reforming. A partial oxidation reaction can occur without removing sulfur and can operate at higher temperatures, 1200°C to 1500°C. (Larminie et al. 2000) This reaction is exothermic and self sustaining once it is initiated. The steam reforming reaction would need a continuous heat source. A common problem in reforming also present in CPOX reforming is having coke build up on the catalyst, therefore deactivating it. To try and reduce the amount of carbon deposition on the catalysts, oxygen-ion conducting catalyst have been used and are better than nickel based catalysts (Shekawat et al., 2006). A study conducted with isooctane using CPOX reforming showed coking is increased when the sulfur content of the fuel is increased. This shows sulfur not only poisons the catalyst, but it also increases coking which deactivates the catalyst quickly (Moon et al. 2004). With the sulfur poisoning the catalyst non-selective reactions will occur causing coking. The catalyst for a CPOX reaction is typically either Ni or Pt. With methane as a fuel, a Ni based catalyst will provide more H₂ but will have a low operation temperature. A Pt catalyst with methane will be more stable but have lower selectivity to hydrogen (Corbo et al. 2006). With a CPOX reaction for a hydrocarbon such as propane, a catalyst with rhodium (Rh) supported on alumina has shown promising results. Pt and Ni catalysts have been studied with many different supports. An aluminum oxide (Al₂O₃) catalyst with supports of nickel oxide (NiO) and calcium oxide (CaO) proved to be superior over a platinum-ceria oxide (Pt-CeO) catalyst for reforming propane. (Corbo et al. 2006) A study was conducted of fuels similar to diesel and jet fuel and for n-Decane and n-Hexadecane over

a Rh-washed monolith. The optimum production of CO and H₂ was at a C to O ratio of 0.8 while the catalyst contact time was 12 ms. The lower the C to O ratio, the higher the temperature of the reaction; therefore a C to O ratio of 0.5 is the lowest C to O ratio the catalyst can handle before it is damaged (Krummenacher et al. 2003).

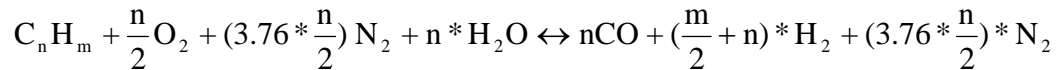
The average pore size of the catalyst can play a large role in producing H₂ and CO. As the pore size increases, the selectivity of H₂ and CO decreases dramatically. A study done on i-octane and n-octane showed the maximum selectivity of hydrogen for an 80 pores per linear inch (ppi) Rh coated alumina foam monolith catalyst is 88% while a 45 ppi foam has a maximum selectivity of 48%. The reason for the decrease in selectivity with the 45 ppi catalyst is more water is produced from the reaction than with the 80 ppi catalyst. (Panuccio et al., 2006) The 80 ppi catalyst has the larger active area leading to higher selectivity to H₂ and CO. For CPOX reactors, many different types of catalysts can be used such as Ni, Pt and Rh. Rh has the best selectivity to hydrogen while not being easily deactivated by aromatics. The Rh catalyst has an advantage over the Pt catalyst since Rh is less likely to produce hydroxyl radicals, thereby producing less water. (Shekhawat et al., 2006). CPOX reactors also reduce the sulfur content in fuels by the following reaction.



This reaction will take hydrogen sulfide (H₂S) and convert it to sulfur, easily separated and removed from the system (Gardner et al. 2002). This is a new approach to desulfurization using sorbent material.

The third method of fuel reforming is a combination of the first two methods.

The idea behind auto-thermal reforming (ATR) is the use of heat from the CPOX reaction as the heat source for the steam reforming, thereby allowing the system to be more efficient (Cheekatamarla et al., 2005). A sample auto-thermal reformation reaction is:



A benefit of auto-thermal reforming is the steam in the system will reduce the carbon deposition a CPOX reactor would normally experience (Shekhawat et al., 2006). In a study conducted on auto-thermal reforming of JP8, it was seen the steam in the reforming process decreased the production of olefins and CO, while the production of hydrogen increased (Dreyer et al., 2006). A study done on ATR of a synthetic diesel fuel showed when using a Pt/Ceria catalyst produced the highest hydrogen yield (79%) when the steam to carbon ratio was 2.5, the O/C ratio was 0.5 and the temperature was 400°C. This study showed synthetic diesel fuel will continue to give a 79% hydrogen yield after 50 hours, thus indicating coking did not occur at these conditions even with aromatics. When JP8 with a sulfur content of 1000 ppmw was tested in this study, it revealed a decrease in hydrogen yield from 75% to 40% over the same period. (Cheekatamarla et al., 2005) This proves ATR with a Pt/Ceria catalyst cannot handle the sulfur contents typically found in military fuels. The problem with ATR is when the catalyst is poisoned by sulfur a decrease in production of hydrogen as well as a decrease in the amount of heat used in the steam reforming.

III. Methodology

Aspen Fuel Processor

The 10 kW Aspen fuel processor is designed to handle jet fuel by desulfurizing the fuel. This experiment operates at a fuel consumption rate of 21 ml/min and an air consumption rate of 68.2 to 75.8 SLPM. The reformer can only handle fuels with up to 1000 ppm of sulfur before H₂ production begins to decrease due to the sulfur poisoning the catalyst. The desulfurization reduces the sulfur build up on the catalyst, preventing the problem of catalyst deactivation. The reformer has eight sulfur absorbent beds heated to 400°C and pressurized to 250-300 psi. The fuel passes through these beds and the sulfur is absorbed. Only six of these sulfur absorbent beds are active at a time while the other two regenerate. Air runs through them to release the sulfur as a mixture of hydrogen sulfide and sulfur oxides back into the fuel tank. This mixture of hydrogen sulfide and sulfur oxide is then vented out of the fuel tank. The switching between active and recharging sulfur absorbent beds is accomplished via a valve between the fuel flow and air flow to the appropriate sulfur absorbent beds. The fuel entering the CPOX reactor is at 350°C to 400°C and exits at approximately 1000°C. If the fuel entering the CPOX reactor gets to higher than 400°C then undesired heterogeneous reaction could occur before the catalyst. The CPOX reactor is a honeycomb structure with a platinum-based catalyst having additives on the catalyst helping to minimize the sulfur build up.

The controller interface for the Aspen reformer was designed in labview. This control panel lets the user see all the values from the temperature and pressure sensors for the desulfurization beds, combustion chamber and CPOX reactor. The user only starts

the reformer and monitors the temperatures and pressure values. Once normal operation levels are achieved then the user can adjust the air flow and fuel flow into the reactor to a desired O/C ratio. The user must monitor the temperature in the CPOX reactor to ensure the temperature will not damage the catalyst or lead to coke formation.

To determine the O/C ratio for the fuel, the fuel density, carbon weight percentage and fuel flow was required. To determine the amount of carbon in moles per minute the following formula was used (shown for JP8 POSF 3773 as an example):

$$\frac{86.1\% * 0.78 \frac{\text{g}}{\text{cc}} * 21 \frac{\text{cc}}{\text{min}}}{12.011 \frac{\text{g}}{\text{mol}}} = 1.174 \frac{\text{moles of C}}{\text{min}}$$

To calculate the amount of oxygen in moles per minute the following equation was used:

$$\frac{72.9 \frac{\text{L}}{\text{min}}}{1000} * \frac{101325 \text{ Pa}}{8.314 \frac{\text{J}}{\text{g mol K}} * 298\text{K}} * 0.209 * 2 = 1.2462 \frac{\text{moles of O}}{\text{min}}$$

This sample calculation gives an O/C ratio of 1.05. These calculations need to be performed to properly adjust the fuel flow and air flow rates to give a desired O/C ratio.

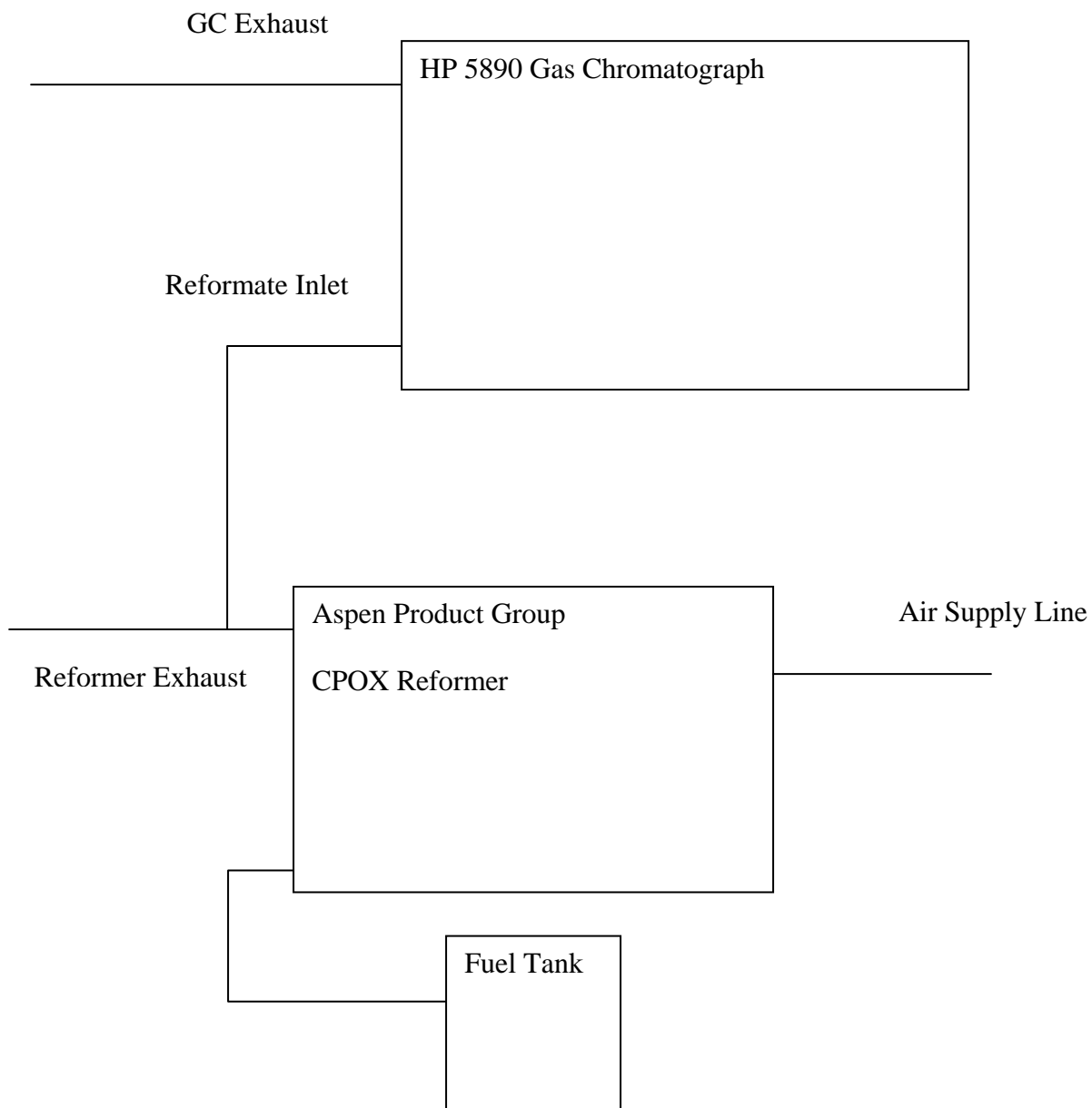


Figure 6: Schematic of experiment setup



Figure 7: Experimental setup

The reformat from the Aspen reformer is sent to the HP 5890 Gas Chromatograph (GC) to analyze the gases. When the reformat exits the Aspen reformer, it enters a T-joint to send a small amount of the reformat to the GC while the rest is sent through a cooling loop and vented out.

The GC will take batch samples of the reformat being produced from the Aspen fuel processor. The two detectors on the GC used to determine the type of gas and the amount gas are the thermal conductivity detector (TCD) and flame ionization detector (FID). The thermal conductivity detector is comprised of a Wheatstone bridge with reference flow over one side of the bridge and sample flow over the other side. The

difference in the reference flow and sample flow can be determined from the temperature change due to thermal conductivity. This thermal conductivity difference will change the temperature and a temperature change will cause a difference in a recorded resistance. The flame ionization detector is a device using an air-hydrogen flame to produce ions. The column sample passes through the flame and burns producing ions. These ions produce an electric current. The more ions created, the greater the signal.

The reformat in the GC is sent through a CTR I column and a Hayesep Q column. The CTR I column is designed to perform at ambient temperatures and separate oxygen, nitrogen, methane, carbon monoxide and carbon dioxide. The CTR I column has an inner column with a 1/8 inch outer diameter, while the outer column has a 1/4 inch outer diameter. The inner column of the CTR I easily separates air, methane and carbon dioxide. The outer column handles oxygen, nitrogen, methane and carbon monoxide. The Hayesep Q column has a polymer composition of divinyl benzene created to separate nitrogen, oxygen, argon, and carbon monoxide at ambient temperatures.

The reformat signals from the GC are compared to signals generated with known gases. Sample gases such as CH₄, N₂, CO₂, CO, and H₂ were sent through the GC to determine at what time peaks in the FID and TCD signal would occur to calibrate the GC for reformat. The TCD will show signals for all the gases to be produced in reformat, except for methane. The FID will help determine the amount of hydrocarbons. The data acquired from the GC were compared with calculations made by Stanjan. Stanjan calculates chemical equilibrium using a method of element potential. Element potential relates mole fractions of each species to quantities referred to as element

potentials. There is one element potential for each independent atom in the system. Stanjan uses the values of absolute entropy at 1 atm and enthalpy values above 298.15 K (25°C). Some of the species needed in this experiment were already in the files for Stanjan, while other species such as n-C₁₀H₂₂, C₁₀H₁₄, a-C₇H₁₄ were added using the accompanying utility JANFILE. These species are used to model JP8 accurately, with a composition of 34% C₁₂H₂₆ 32% C₁₀H₂₂ 15% C₁₀H₁₄ 16% C₇H₁₄ 4% S (Montgomery et al. 2002). The Burcat database provided the values for enthalpy and entropy. This database provided the data in a polynomial form, allowing the values of enthalpy and entropy to be calculated for different temperatures. These values had to be entered into the JANFILE program. The new species could then be used in Stanjan to perform the chemical equilibrium calculations. Calculations were made for fuels with different percentages of aromatics. Aromatics should produce more coking issues since the bonds will be difficult to break and lead to coking or coking precursors. This is of interest to see how this would affect the reformation process. These calculations will be helpful in determining an ideal operating condition based on how different species changes with temperature and O/C ratios.

Error estimates

There are two major components in the testing system to determine systemic error. The first is the mass flow controller. With flows from 68.2 SLPM to 75.8 SLPM the mass flow controller was observed varying from the set point. The other systemic error is with the fuel pump. With normal fuel flow at 21 cc/min, the fuel flow was measured at times being less than or greater than the set point. These two systemic errors

will contribute to the O/C ratios varying. The systemic error in the data could contribute to the statistical error by varying the O/C ratio from the set point and causing the values of mole fractions to increase or decrease. The statistical error was measure by determining the standard deviation for the values measured at each O/C ratio for all the reformat components (Table 1).

The mass flow controller flow varied up to 0.5 SLPM from the set point. The fuel pump flow would vary 0.2 cc/min. The pump flow variation was measured by disconnecting the flow into the desulfurization beds and having the fuel flow into a graduated cylinder for a set time period with a set flow. This variation leads to JP8 with 700 ppm sulfur having the O/C ratio plus or minus 0.018. JP8 with 400 ppm will have an O/C ratio that varies plus or minus 0.0172 and S8 will be plus or minus 0.0182. The standard deviation of the values recorded for each O/C ratio is in Table 1.

Table 1: Standard deviation of reformat mole fraction values

Fuel	O/C ratio	H2	CO	CO2	N2
JP8 700	1.05124	0.00336	0.00767	0.00132	0.00829
JP8 700	1.07576	0.00387	0.00739	0.00079	0.00620
JP8 700	1.10027	0.00543	0.00787	0.00171	0.00406
S8	1.05508	0.00869	0.01393	0.00188	0.01211
S8	1.07519	0.00504	0.00957	0.00116	0.00845
S8	1.10458	0.01011	0.01361	0.00146	0.01305
JP8 400	1.05008	0.00544	0.00664	0.00151	0.00727
JP8 400	1.07477	0.00420	0.00953	0.00119	0.01018
JP8 400	1.10092	0.00552	0.01618	0.00208	0.01646

Table 2: Percent error of mole fraction reformat values

Fuel	O/C	H2 (%)	CO	CO2	N2
JP8 700	1.051	1.473	3.131	17.303	1.598
JP8 700	1.076	1.697	3.085	11.469	1.181
JP8 700	1.100	2.428	3.319	21.968	0.764
S8	1.055	3.601	6.043	20.461	2.334
S8	1.075	2.057	4.234	13.304	1.624
S8	1.105	4.058	6.318	16.020	2.479
JP8 400	1.050	2.329	2.783	20.513	1.397
JP8 400	1.075	1.843	4.012	16.092	1.930
JP8 400	1.101	2.529	6.822	21.699	3.078

The largest uncertainty is for carbon dioxide since it is the smallest component in the reformat. The lowest occurs for O/C values of 1.075 due to three to four hours of testing at each of those points versus the other points with testing of one hour.

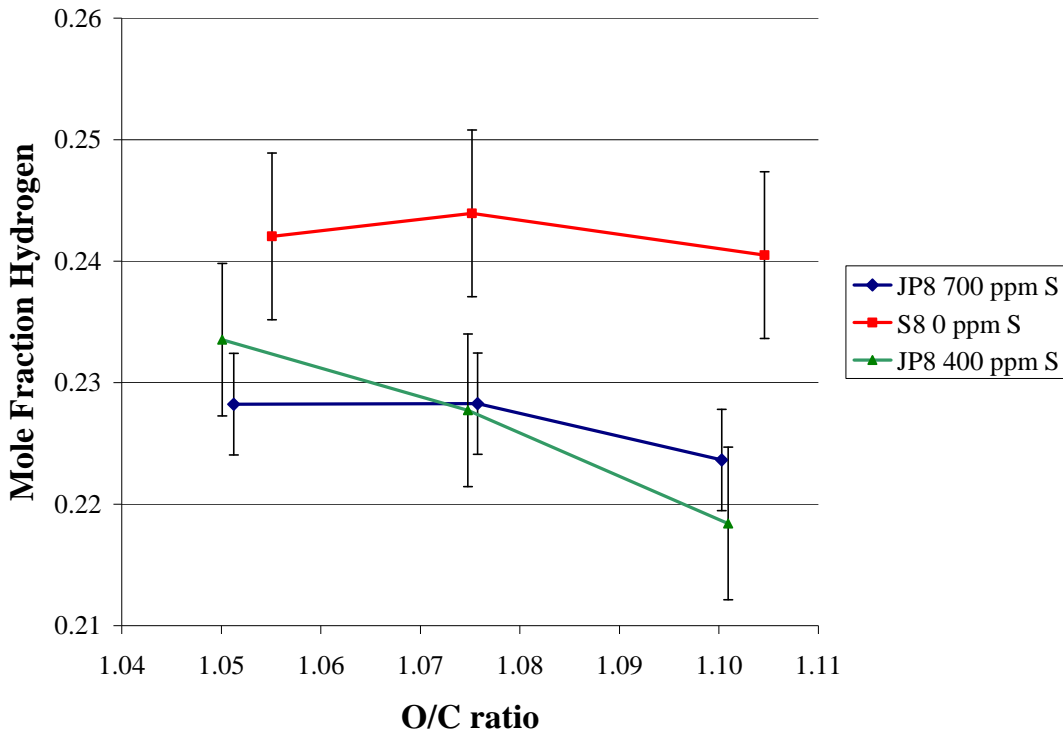


Figure 8: Hydrogen varying O/C ratio with statistical error

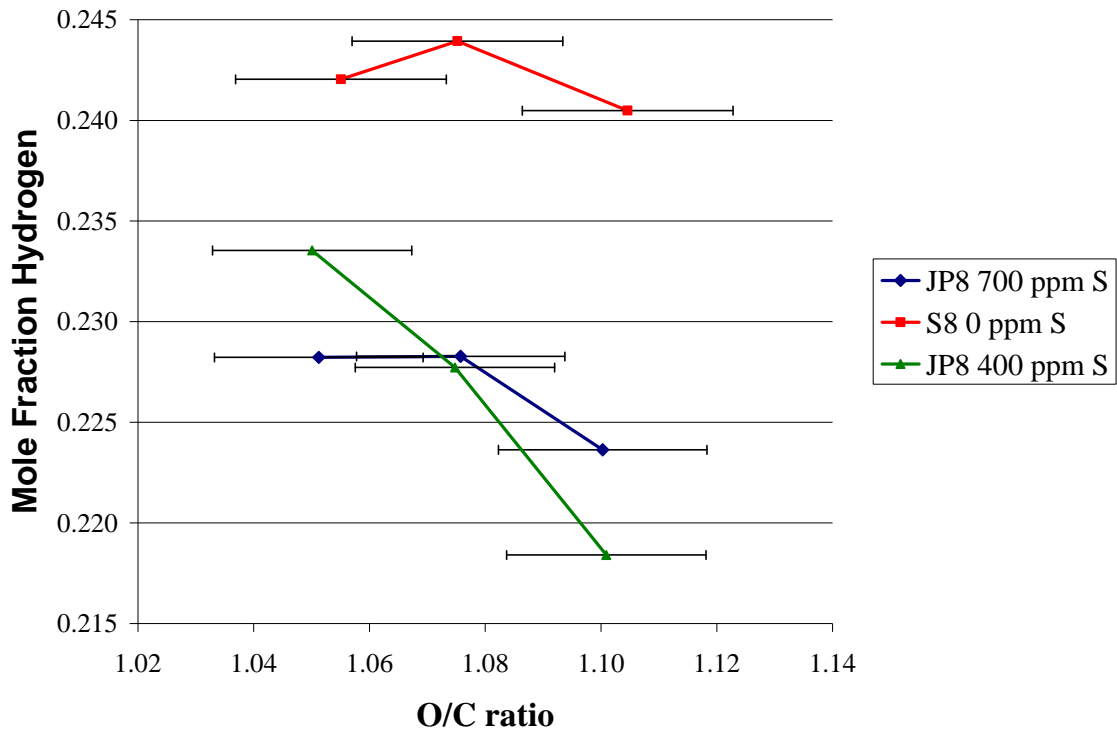


Figure 9: Hydrogen varying O/C ratios showing O/C ratio systematic uncertainty

Figure 8 and 9 are samples of the statistical and systemic error for these calculations.

Plots of other reformate products with error bars can be found in the appendix. The error bars are not present in the plots later in this paper in an attempt to make the plot easier to read and enhance understanding of the data presented.

IV. Analysis and Results

Results from Stanjan Simulations

The 31% aromatics was a starting point since Montgomery et al., 2002 suggested JP8 is composed of 34% C₁₂H₂₆ 32% C₁₀H₂₂ 15% C₁₀H₁₄ 16% C₇H₁₄ 4% S. The percent of aromatics was varied to see how it would affect the output. Without creating a chemical kinetic mechanism, changing aromatics had very little effect on the chemical equilibrium calculation. A study was performed using experimental data to help explain the surface kinetics of the system since the largest hydrocarbon with surface kinetics data available is ethane. This same study used a plug flow subroutine in Chemkin to handle the homogeneous calculation for the CPOX reactor (Panuccio et al., 2006).

The difference in hydrogen selectivity is approximately 1% between 60% aromatics and 0% aromatics. These predictions show S8 (0% aromatics) should produce more hydrogen than JP8 (31% aromatics). This shows the highest predicted hydrogen selectivity will occur at 800°C. For higher aromatics the decrease in H₂ leads to an increase in methane.

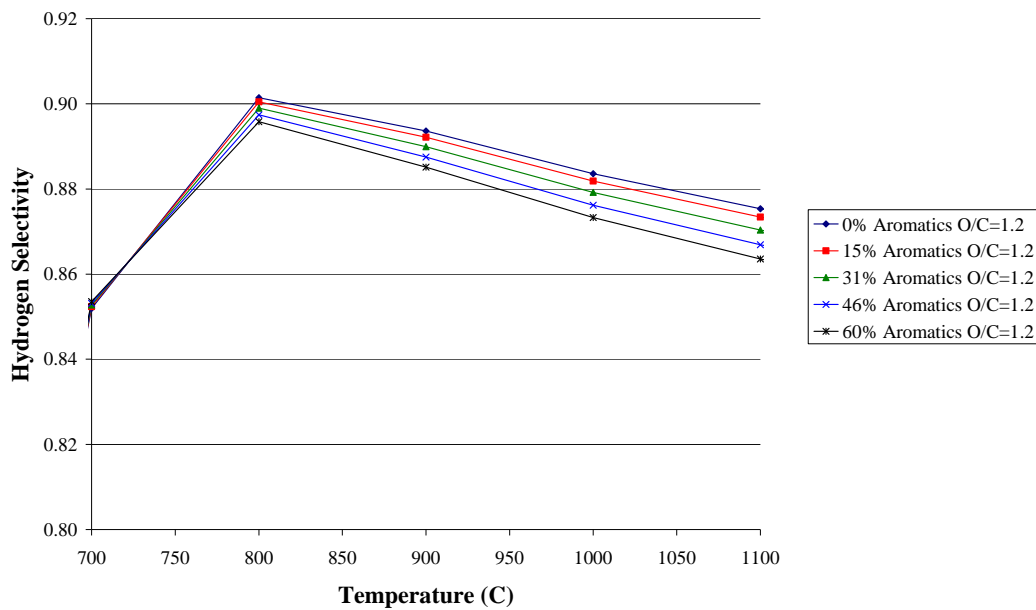


Figure 10: The effects of aromatics on hydrogen selectivity with respect to temperature

The carbon selectivity for C for different aromatics does not change the effects of coking. There is a large decrease in coking from 600°C to 700°C (Figure 11).

Aromatics should produce more coking issues since the bonds will be difficult to break and leads to coking or coking precursors. For an O/C ratio of 1.2 as shown in the graph the operating temperature should be above 800°C to eliminate coking.

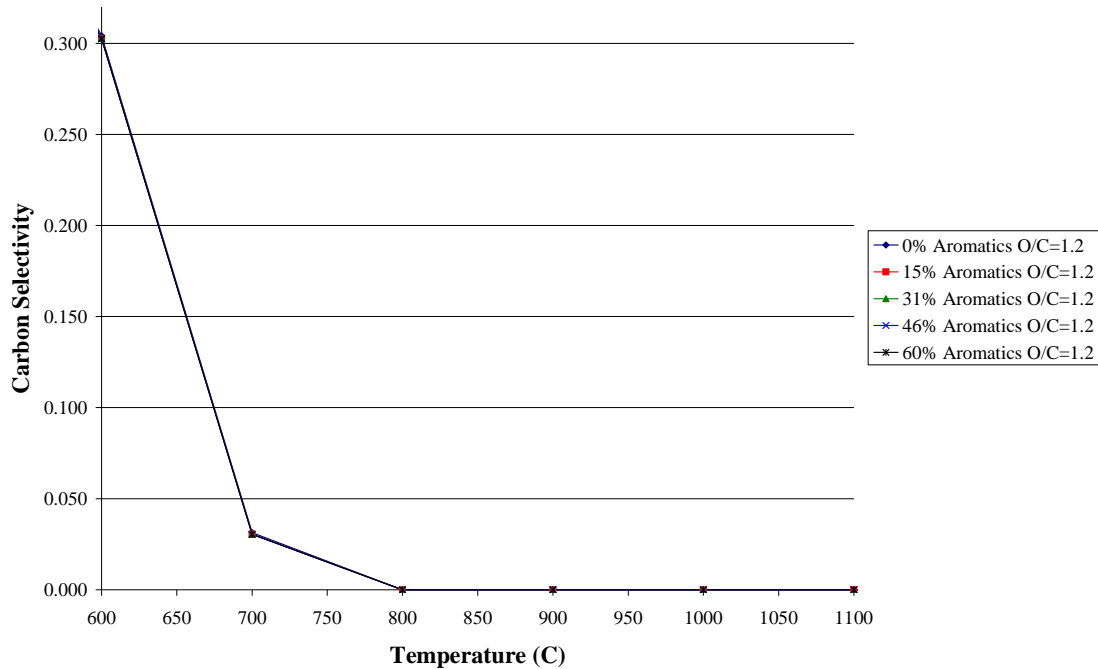


Figure 11: The effects of aromatic on coking with respect to temperature

Changing the O/C ratio had a big impact on hydrogen and carbon selectivity for JP8. H₂ with varying O/C ratios, and temperatures in the range of 700°C to 800°C showed different effects. At 700°C and an O/C ratio of 1.4 the hydrogen production begins to vary from all the other O/C ratios. At 800°C the hydrogen selectivity at an O/C ratio of 1.2 is varying from all other O/C ratios. When at 800°C, the difference in hydrogen selectivity from an O/C ratio of 1 to 1.4 is 13% to 15% depending on the aromatics composition. The difference in hydrogen selectivity between O/C ratios of 0.6 and 1 is only 0.4% (Figure 12). Having an O/C ratio of 1 or less will yield more hydrogen. Between 600°C to 800°C there is a large increase in hydrogen. The higher O/C ratios have lower hydrogen selectivity due to the selectivity to H₂O increasing. Higher hydrogen selectivity leads to higher efficiency for the system

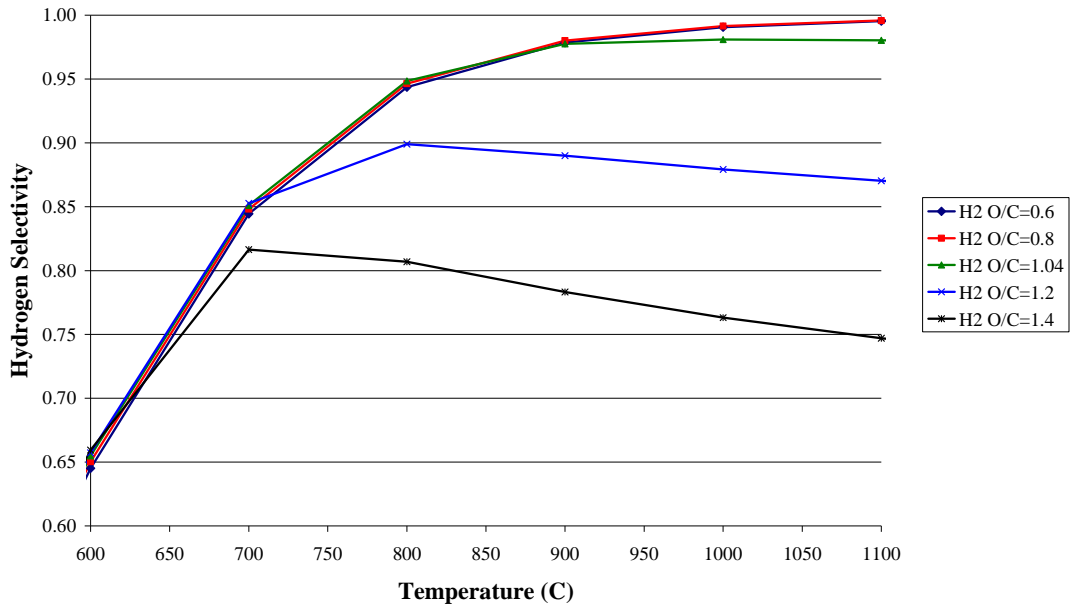


Figure 12: Effect of varying O/C ratio on the production of hydrogen with respect to temperature

For C, the carbon selectivity will decrease as you increase the O/C ratio and temperature (Figure 13).

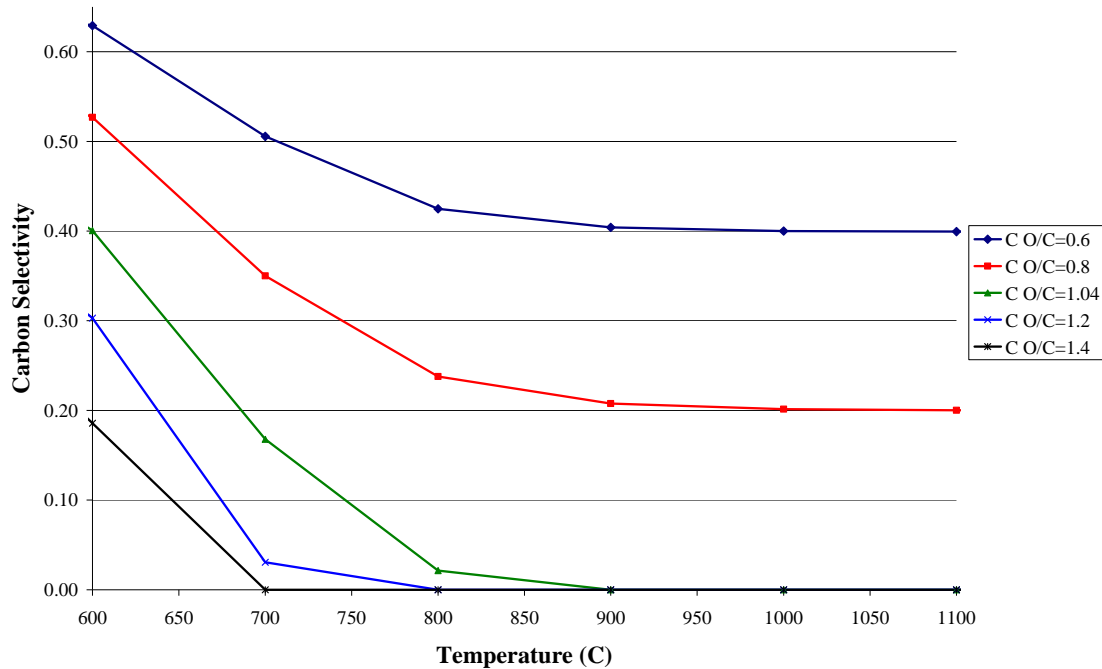


Figure 13: The effects of varying O/C ratios on coking with respect to temperature

This figure shows the dramatic decrease in carbon over the temperatures from 600 to 800° C for JP8. O/C has an important role in reducing coking. The reformer is designed to run at an O/C ratio between 1.0 and 1.1. To reduce coking issues the reformer should be above 950°C to ensure coking will not occur. With O/C higher than 1.0 the excess carbon will lead to more coking occurring. To produce the maximum amount of H₂ while producing the lowest amount of C, the ideal system would be run at 950° C with an O/C ratio a little above 1.0. For the ideal system, the expected carbon output would be 1% CH₄, 0% C, 4.5% CO₂ and 94.5% CO. The hydrogen output in the ideal system

would be 1.5% CH₄, 4.1% H₂O and 94.4 % H₂ (Figures 14 and 15)

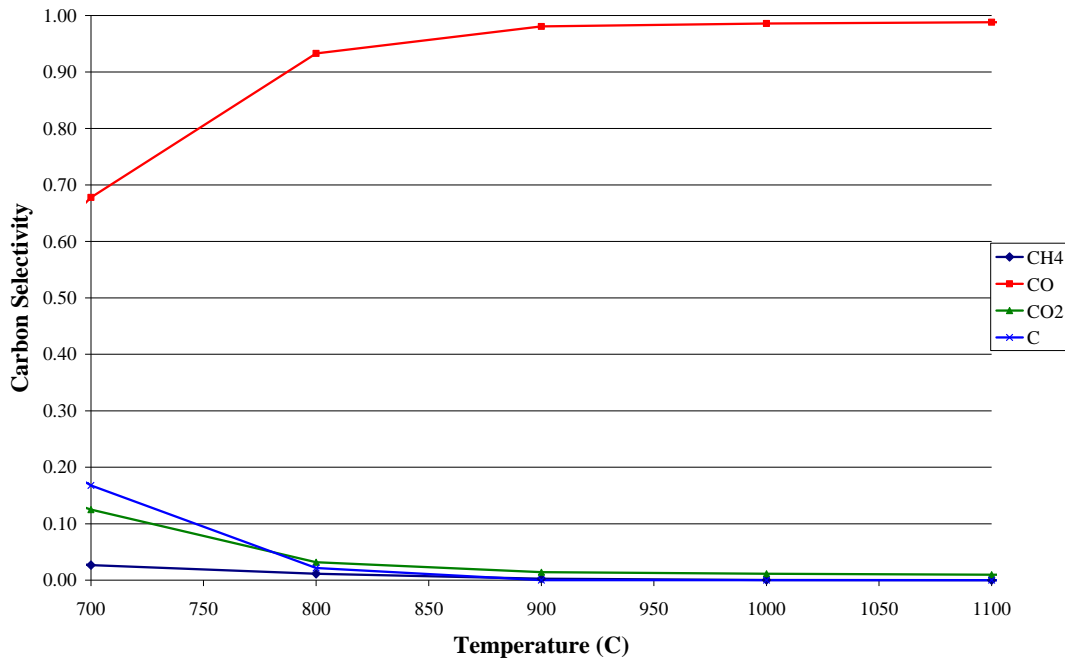


Figure 14: Major carbon products with an O/C ratio of 1.04 with respect to temperature

Figure 14 shows the selectivity to CO increases with temperature for JP8. Increasing the O/C ratio will increase CO₂ while decreasing coking and methane. Coking and carbon dioxide are undesired products. Carbon dioxide will drive down the systems efficiency since CO is a desired product and provide thermal energy. If carbon dioxide is produced then the CO selectivity will be decreasing. The desired operation point is at an O/C ratio of 1.0 providing a temperature of 1000°C.

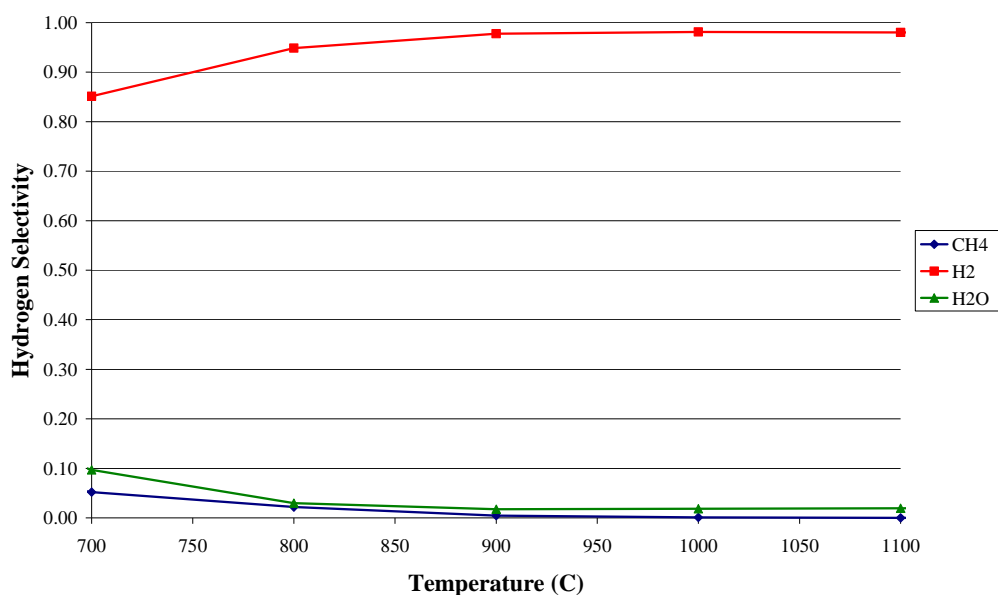


Figure 15: Major hydrogen products with an O/C ratio of 1.04 with respect to temperature

Figure 15 shows the selectivity to H₂ increases with temperature for JP8. For increasing O/C ratios methane will decrease while H₂O increases. Water is an undesired product since it will decrease the amount of hydrogen produced. Ideally the system would run at an O/C ratio of 1.0 and a temperature of 1000°C to minimize the selectivity to water and maximize the selectivity to hydrogen.

These are equilibrium calculations at an ideal point; thus, the actual results of a system such as this will vary. These plots show a temperature of around 900° C to 1000° C will create the highest CO and H₂ selectivity. Running at any temperatures higher than this will slightly decrease the hydrogen selectivity and only improve the CO selectivity by 0.4%. By running at a higher temperature the catalyst could be damaged due to the

heat. To decrease the amount of CH_4 , a high O/C ratio and temperature are required. A decrease in CH_4 is desired because it indicates the dehydrogenation reactions are decreasing, which is associated with lower coking rates (Figure 16).

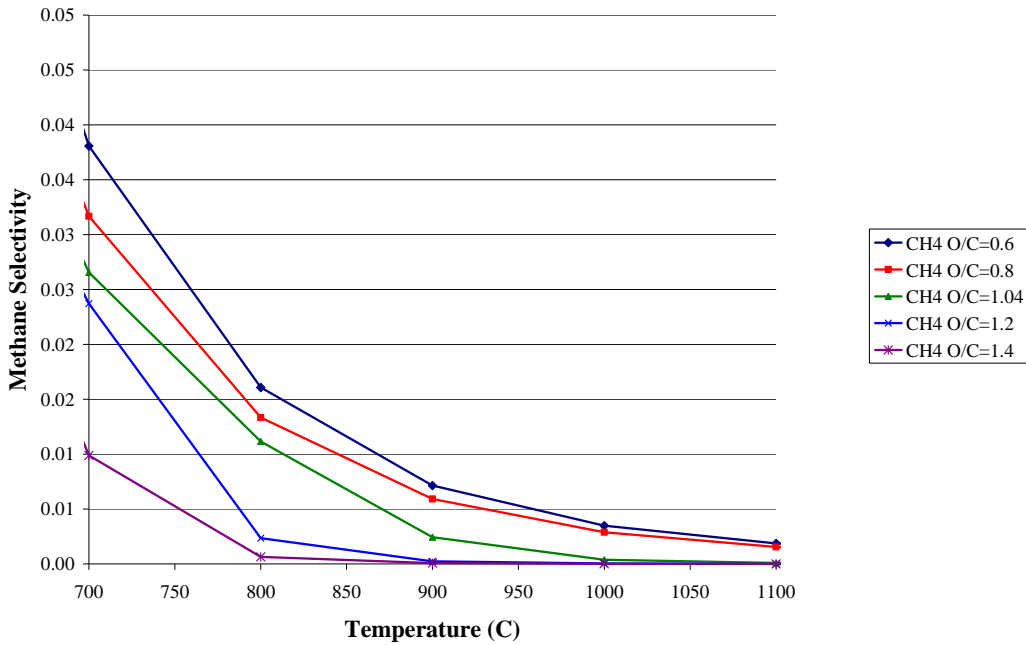


Figure 16: Carbon selectivity to methane with varying O/C ratios with respect to temperature

In order to lower the amount of H_2O , a high O/C ratio and high temperature is required. H_2O is not a desirable product since it will be taking some of the hydrogen away from the production of H_2 (Figure 17). To minimize water production running at an O/C ratio of 1.0 and a temperature of 1000°C would be ideal.

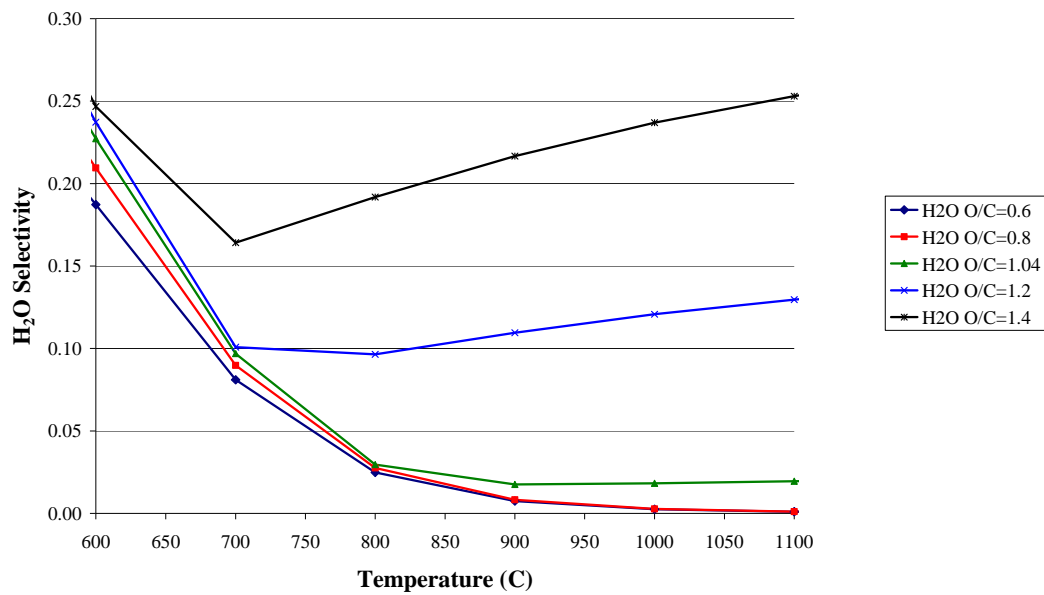


Figure 17: Hydrogen selectivity to water varying O/C ratios with respect to temperature

To decrease the amount of CO_2 , a low O/C ratio and a high temperature are needed. CO_2 reduction shows that the Boudouard reaction is reduced and the amount of coking is in turn reduced (Figure 18).

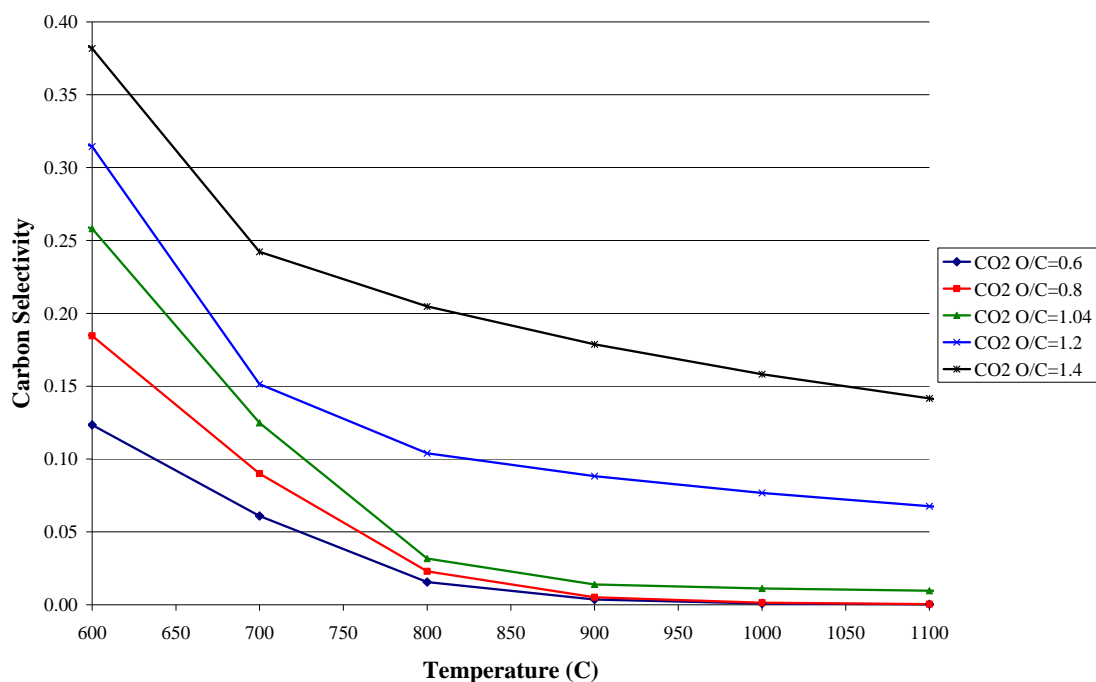


Figure 18: Carbon selectivity to carbon dioxide with varying O/C ratio with respect to temperature

CO seems to have a similar pattern as H₂ between 600° C to 800° C, the carbon selectivity to CO increases 65%. The highest selectivity is at an O/C of 1.04 and the carbon selectivity to CO only increases 0.4% from 1000°C to 1200 C° showing operation at 1000°C is ideal to reduce the damage to the catalyst from the high temperatures. This is somewhat expected since the stoichiometric balanced equation would yield only CO and H₂. CO is a desired product and can be used to power SOFC and MCFC. Higher CO selectivity leads to higher efficiency for the system. Increasing O/C ratios will produce more carbon dioxide while decreasing coking and methane (Figure 19).

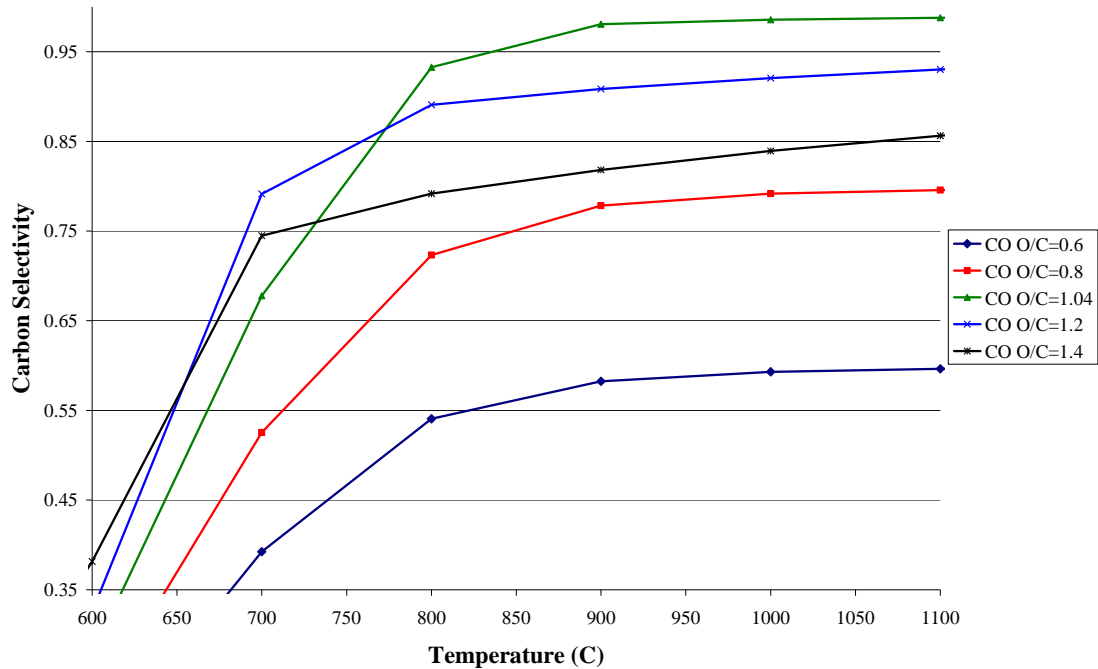


Figure 19: Carbon selectivity to carbon monoxide with varying O/C ratios with respect to temperature

Some coking precursors such as C_2H_2 , C_2H_4 , C_3H_2 , C_3H_4 , C_3H_4O and C_3H_6 were examined using Stanjan. With the Aspen reformer non-methane hydrocarbons should be less than 0.2% mole fraction of the reformat. With such a small concentrations of non-methane hydrocarbons, these could not be found with the flame ionization detector when the signal was integrated. The results showed between 600°C and 800° C, all the coking precursors increased when the O/C ratio was 1.0 or below. Having O/C ratios at 1.2 or above will cause all coking precursors to decrease or level off at temperatures between 600°C to 900° C. The coking precursors do not comprise a significant portion of the carbon output because the largest carbon selectivity at the ideal point of 1000°C and O/C ratio of 1.04 would be 0.0000171% of C_2H_4 (Figure 20).

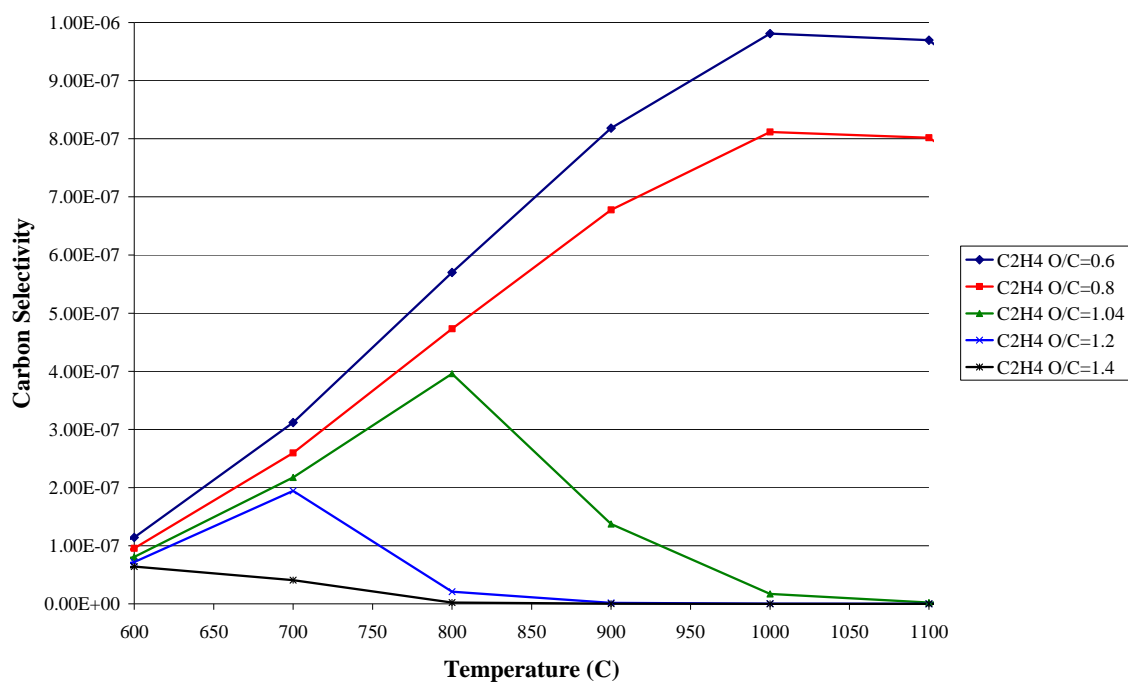


Figure 20: Carbon selectivity to ethylene with varying O/C ratios with respect to temperature

The significance of the coking precursor is to observe trends, take note of where these form and discover how they might break down and cause coking. Sulfur selectivity shows the sulfur in the system will bond with CO to form COS. Once the temperature is above 700° C, COS begins to decrease while S₂ begins to increase. This could also be used to explain the increase in CO from 600°C to 800°C (Figure 21).

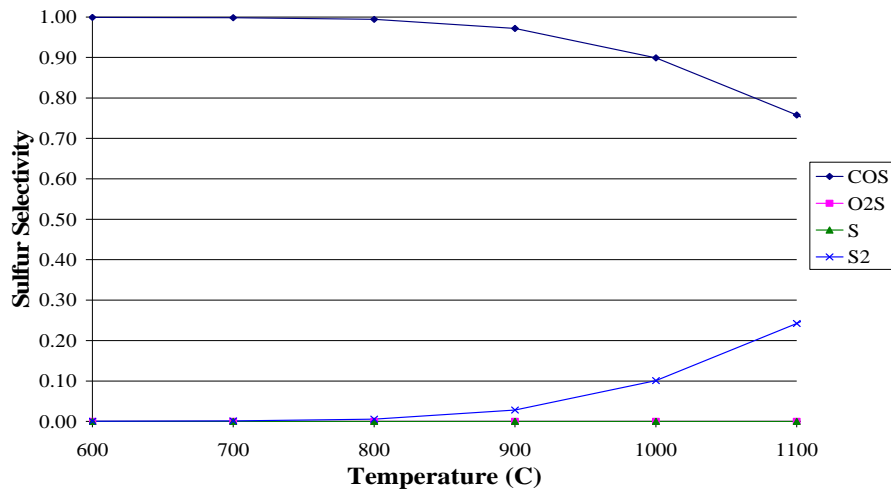
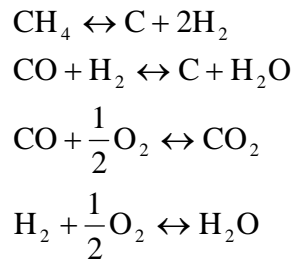


Figure 21: Sulfur selectivity for the major sulfur products at 31% aromatics and O/C ratio of 1.04 with respect to temperature

Some reactions that are undesirable are shown below:



The reactions above either cause coking or will take a desired product of CO and H₂ and convert it into an undesirable product. The design points for the reformer with JP8 fuel are shown in Table 3. Table 3 shows the reformer should be used at an O/C ratio of 1.04 and a temperature of approximately 1000°C.

Table 3: Stanjan predictions for design point using JP8

STANJAN	O/C	Temperature
Maximize H2	1.04	1000
Minimize Coking	1.04	950
Maximize CO	1.04	1000
Minimize CO2	0.6	900
Maximize Efficiency	1.03	1000

Results from Aspen Reformer

The goal of this study is to determine if S8 could be used as a fuel in fuel reforming. This study will look at the effects of aromatics and sulfur concentrations on the systems efficiency and production of desired reformat products (hydrogen and carbon monoxide). The O/C ratios will be varied from 1.05 to 1.1 to determine the design point for each fuel. This data will be compared to the chemical equilibrium data to analyze how the system performed.

The fuels tested were JP8 POSF 3773, JP8 POSF 4751 and S8 POSF 5018D. These three fuels have varying sulfur contents of 0 ppm (S8), 400 ppm (JP8 POSF 4571), and 700 ppm (JP8 POSF 3773). The fuel density of S8 is 0.747 g/ml while both JP8 fuels have a density of 0.78 g/ml. The carbon content by percent mass is lowest in S8 with a value of 84.6 %. JP8 POSF 3773 has a carbon content of 86.1% and JP8 POSF 4751 has a carbon content of 86.3%. The percent of aromatics varied vastly for these three fuels. JP8 POSF 3773 has 15.9% aromatics, JP8 POSF 4751 has 21% aromatics and S8 has zero aromatics.

Mass balances were performed to help determine how much of the fuel was converted into reformat distinguishable by the gas chromatograph. To do this, the moles

of nitrogen per minute and hydrogen per minute were calculated in a similar manner as above.

$$\frac{13.9\% * 0.78 \frac{\text{g}}{\text{cc}} * 21 \frac{\text{cc}}{\text{min}}}{1.00794 \frac{\text{g}}{\text{mol}}} = 2.25888 \frac{\text{moles of H}}{\text{min}}$$

$$\frac{72.9 \frac{\text{L}}{\text{min}}}{1000} * \frac{101325 \text{ Pa}}{8.314 \frac{\text{J}}{\text{g mol K}} * 298\text{K}} * 0.78 = 2.3255 \frac{\text{moles of N}_2}{\text{min}}$$

To calculate the mass into the system, the moles for C, O, H, and N can be multiplied by their molecular weight to give the units of grams per minute. The gas chromatograph is set to take a sample for one minute; therefore, the sum of grams per minute for each element is equal to the mass into the system. To determine the mass out of the system, nitrogen must be used as a tie component since it should not react with anything. A tie component should not change going through the reformer. The amount of nitrogen into the reformer will match the nitrogen leaving the reformer. The total moles out of the system can be determined by taking the total moles of nitrogen into the system and multiplying it by one over the mole fraction of nitrogen from the gas chromatograph reading as shown in the equation below.

$$2.3255 \frac{\text{moles of N}_2}{\text{min}} * \frac{1}{.5254 \text{ mole fraction}} = 4.42615 \text{ total moles out of system}$$

Once the total moles have been determined, multiplying the total moles by the mole fraction will supply the moles of each component. Then multiplying the molecular

weight by the amount of moles will give the mass of each component. The mass of each component is summed to calculate the mass out of the system. The mass balance is just mass out of the system divided by the mass into the system. The mass balance calculations for the system ranged from .9119 to 1.000.

With the values of O, C, H and N₂ being determined in moles per minute a simple conversion from moles per minute to grams per minute is necessary for efficiency calculations as shown in the equation below.

$$1.174 \frac{\text{moles of C}}{\text{min}} * 12.011 \frac{\text{grams}}{\text{mole}} = 14.101 \frac{\text{grams}}{\text{min}}$$

This same calculation is performed to convert moles of hydrogen per minute to grams of hydrogen per minute. The lab test reports for each fuel give the heat of combustion of the fuel in terms of BTU/lb.

Table 4: Heats of Combustion for fuels and reformat

	Heat of Combustion BTU/lb	Heat of Combustion MJ/Kg
JP8 POSF 3773	18625	43.322
JP8 POSF 4751	18584	43.226
S8 POSF 5018D	18964	44.110
H2	60957.7	141.788
CO	4343.6	10.103

To simplify the calculations, this was converted into MJ/kg and the energy into the system was calculated with the following equation.

$$43.226 \frac{\text{MJ}}{\text{kg}} * \left(\frac{14.101 \text{g}}{1000} + \frac{2.27552 \text{g}}{1000} \right) = .70789 \frac{\text{MJ}}{\text{min}} = 11.798 \text{ kW}$$

To determine the energy out of the system, the moles for CO and H₂ are multiplied by their respective molecular weight to give the amount of CO and H₂ in grams. An example

is 0.9276 moles of H₂ and 0.9274 moles of CO used to calculate energy out of the system using the heats of combustion for CO and H₂ (Perry, et al. 1973).

$$\frac{30.3758 \text{ grams of CO}}{1000} * 10.103 \frac{\text{MJ}}{\text{kg}} + 141.788 \frac{\text{MJ}}{\text{Kg}} * \frac{2.0885 \text{ grams of H}_2}{1000} = 0.6030 \frac{\text{MJ}}{\text{min}} = 10.05 \text{ kW}$$

To determine the efficiency, the energy out of the system is divided by the energy into the system as shown below.

$$\frac{10.05 \text{ kW}}{11.798 \text{ kW}} = .8518$$

The FID results from the Aspen reformer data show JP8 with 400 ppm of sulfur produces 2.4 times the amount of methane than S8 produces, while JP8 with 700 ppm of sulfur produces 4.25 times more methane than S8 produces. Mole fraction data could not be calculated due to methane not showing up in the TCD data. This difference in the amount of methane produced can be attributed to the differences in sulfur. Since S8 has zero aromatics, it is easy to breakdown to CO and hydrogen without making any methane. With the sulfur contents being so different, it is expected the higher sulfur content fuel will produce the least amount of hydrogen due to the sulfur poisoning the catalyst. As sulfur content increases, the production of hydrogen decreases (Figure 22). S8 proved to provide the highest hydrogen production. The difference in mole fraction of hydrogen between both JP8 fuels is only 0.01%. S8 produced the largest amount of hydrogen due to having the highest weight percentage of hydrogen for all the fuels tested. The difference in hydrogen could be attributed to aromatic composition of the fuels, S8

has 0% aromatics while JP8 with 400 ppm S has 21% and JP8 with 700 ppm S has 15.9%.

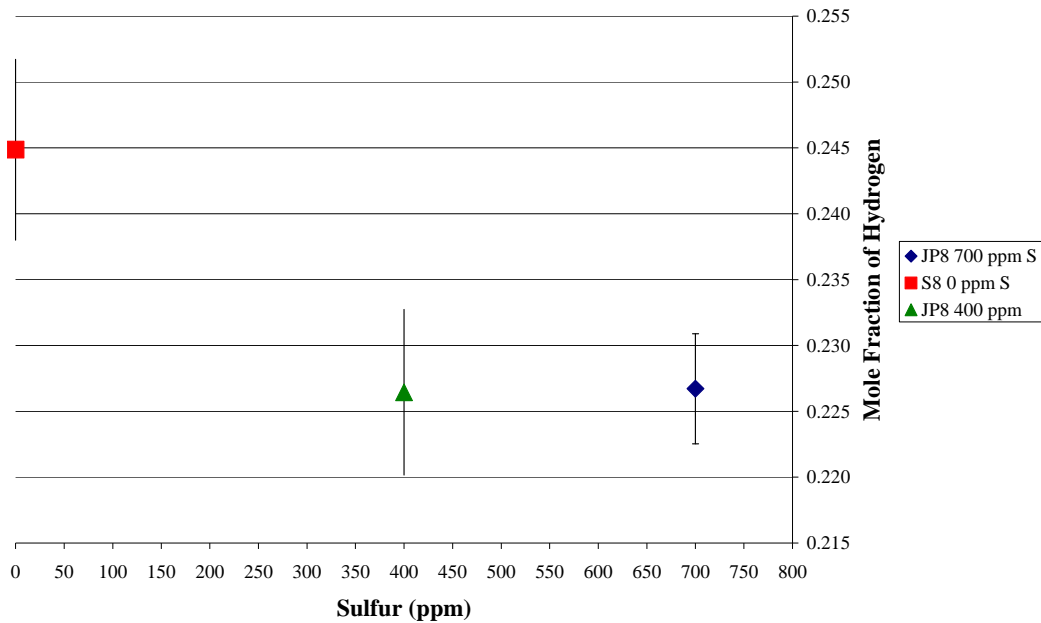


Figure 22: The effects of sulfur content in fuels on the production of hydrogen

Figure 22 shows sulfur content did not have a dramatic effect on the hydrogen production. Since the reformer contains desulfurization beds to remove the sulfur from fuels with up to 1000 ppm of sulfur, this difference in hydrogen production could be attributed to the fact S8 has 0% aromatics while JP8 has 15.9% and 21% aromatics. The desulfurization beds in the Aspen reformer help keep the hydrogen steam constant over a long period of time without the catalyst getting poisoned from sulfur content in the fuels (Figure 23).

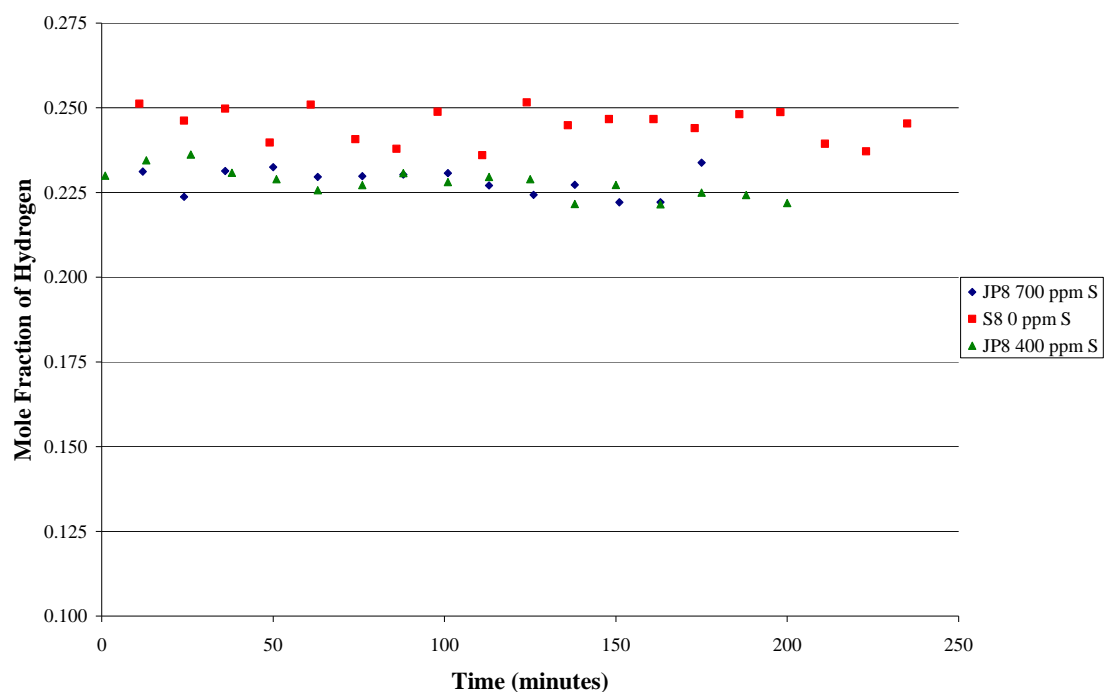


Figure 23: Constant hydrogen production over a long period of time with fuels of various sulfur levels

The difference in hydrogen weight percentage is the most likely cause for this difference in hydrogen production. S8 is 15.4% hydrogen by weight and both JP8 fuels are 13.7% and 13.9%. Therefore, the more hydrogen in the fuel, the more hydrogen one can expect out of the reformer (Figure 24).

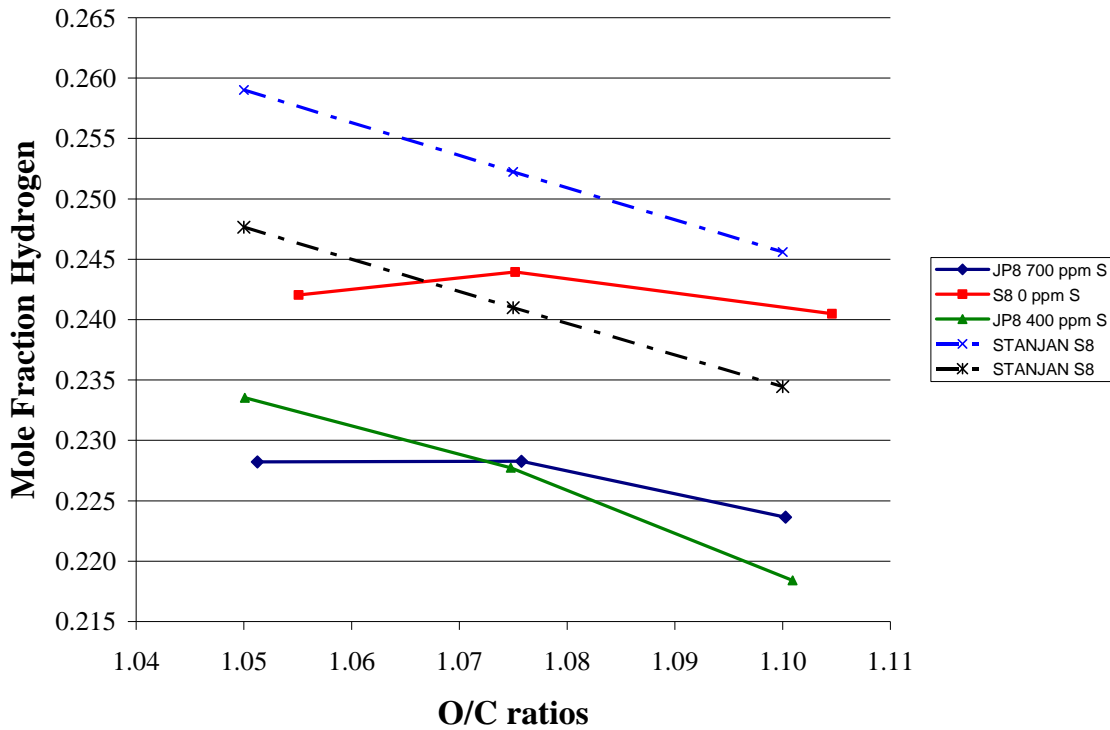


Figure 24: The effects of varying O/C ratios on the production of hydrogen with various fuels and modeled fuels

Through analysis of the data, the design point for S8 and JP8 with 700 ppm sulfur is an O/C ratio of 1.075. The JP8 with 400 ppm had the highest temperature for the CPOX reactor at each O/C ratio. The O/C ratio allows for adjustment of the temperature in the CPOX reactor; therefore, since JP8 with 400 ppm has the highest temperature, a design point shift to a lower O/C is logical. With S8 having the highest hydrogen weight percentage it was predicted and expected S8 would produce more hydrogen than either JP8 fuel. The predicted difference in hydrogen for S8 and JP8 is 0.0113% and the actual difference is 0.0155%.

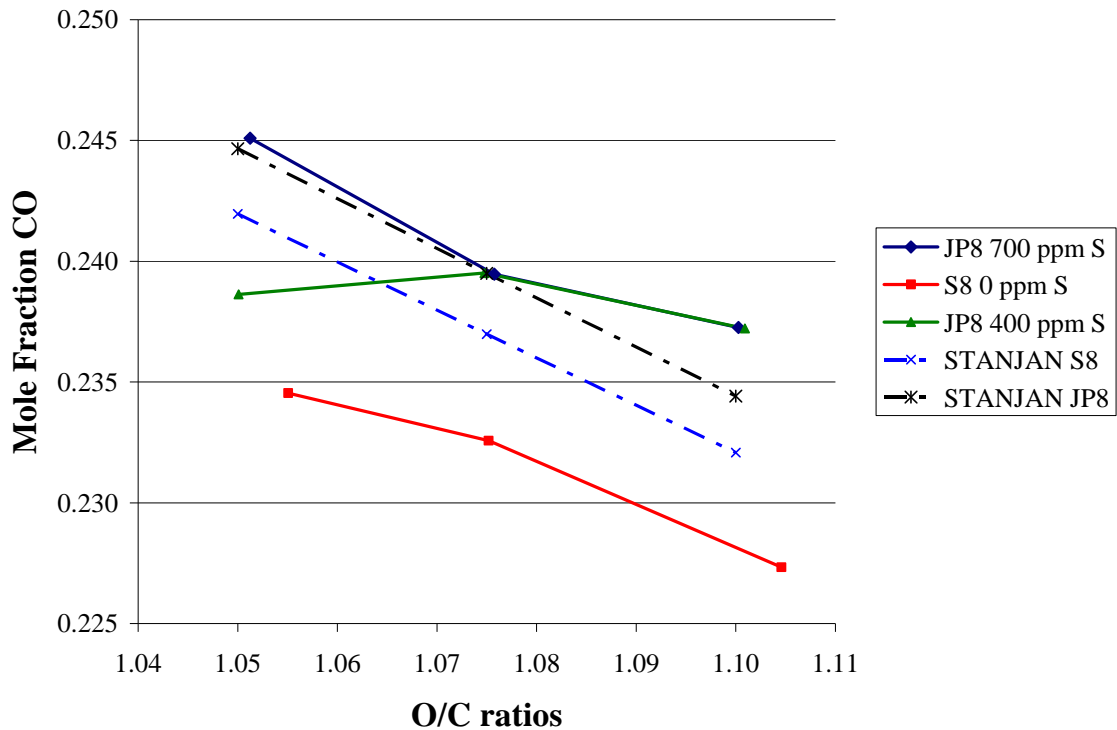


Figure 25: The effects of varying O/C ratios on the CO production with various fuels and modeled fuels

All fuels have similar trends to the modeled fuels. The JP8 with 400 ppm sulfur produces the least amount of CO of the two fuels due to the fact it has a higher percent of aromatics (21%) as compared to JP8 with 700 ppm sulfur (15.9%). It is expected and predicted for S8 to have lower CO production (0.0025%) than JP8 due to the lower carbon weight percentage value of S8 versus JP8. The actual difference for CO mole fraction is 0.007%. S8 should have a lower amount of CO due to the lower carbon weight percentage as compared to JP8. S8 has a carbon weight percentage of 84.6% as compared to JP8 with 400 ppm sulfur at 86.3% and JP8 with 700 ppm sulfur at 86.1%. (Figure 25)

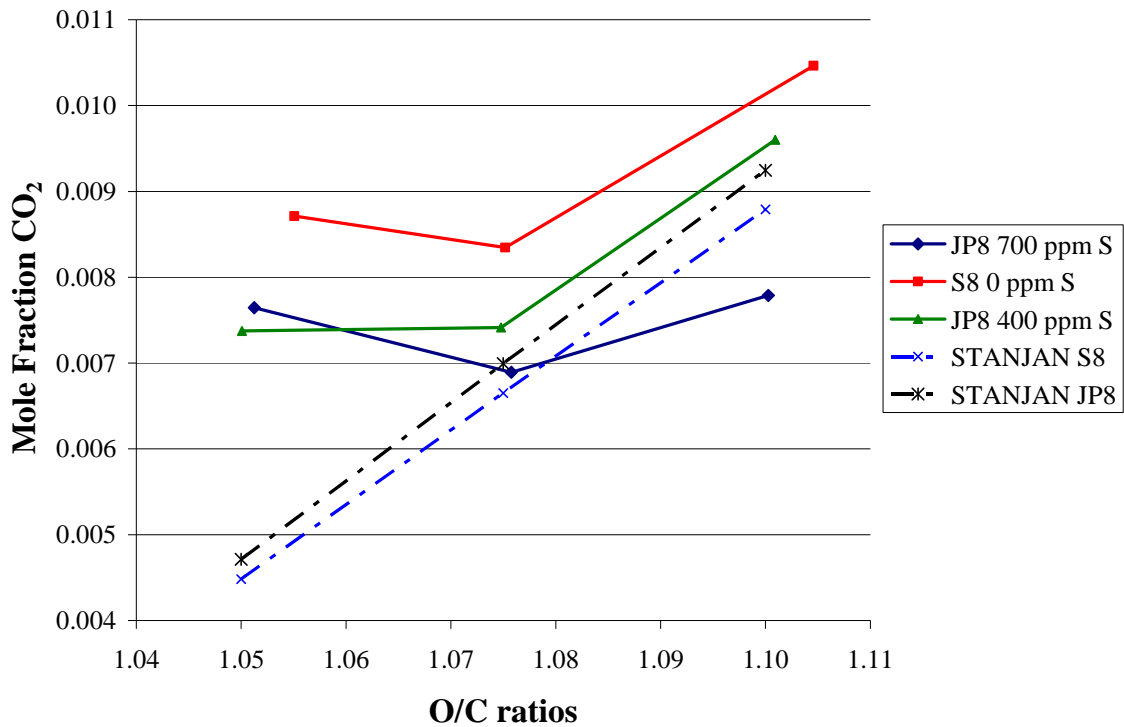
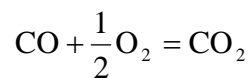


Figure 26: The effects of varying O/C ratios on the CO₂ production with various fuels and modeled fuels

Due to the fact S8 has a lower CO mole fraction than the JP8 fuels, it is logical for S8 to have more CO₂. (Figure 26) This is due to a reaction that was addressed earlier.



This reaction is not desirable since carbon dioxide will lower the efficiency values for the system. The expected efficiency from the reformer predicts S8 should outperform the JP8 fuels in efficiency due to S8 having no aromatics. (Figure 27)

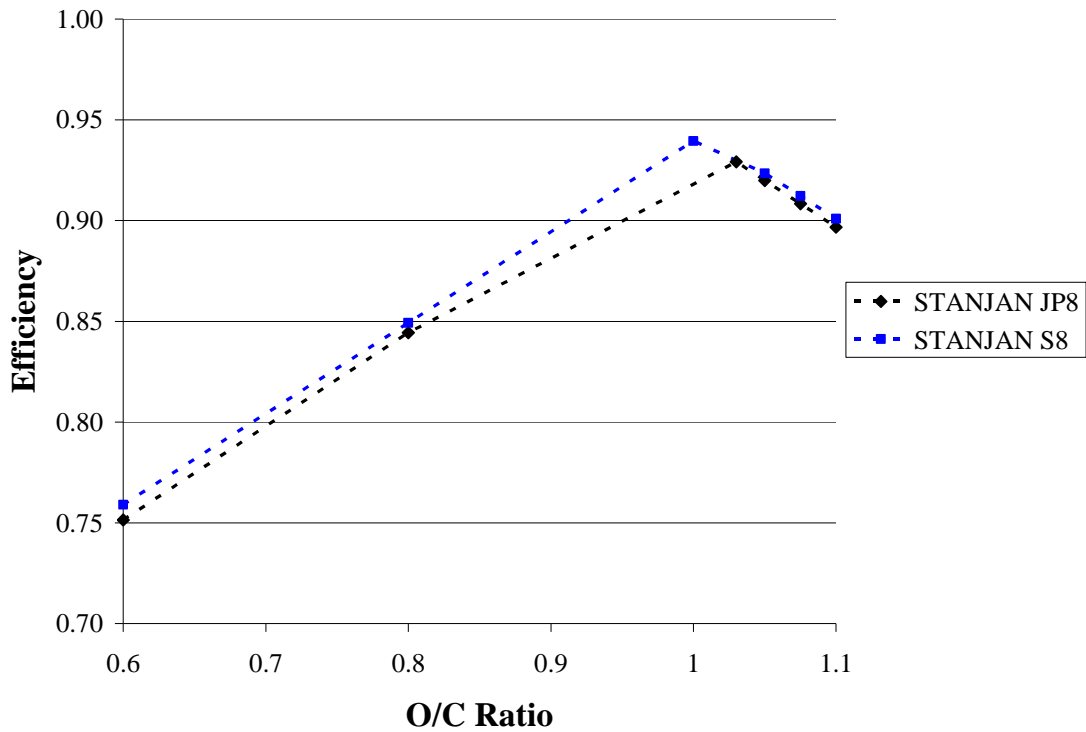


Figure 27: Predicted efficiency for the Aspen reformer using JP8 or S8 with respect to O/C ratios

By inspection of Figure 27, the design point for the reformer from the Stanjan calculations is around 1.0 to 1.03 at a temperature of 1000°C. The highest efficiency for S8 is 94% and JP8 is 92.9%. The samples of JP8 and S8 used with the reformer were run with O/C ratios varying from 1.05 to 1.1. The reformer was designed to run at an O/C ratio of 1.075 to produce optimal results.

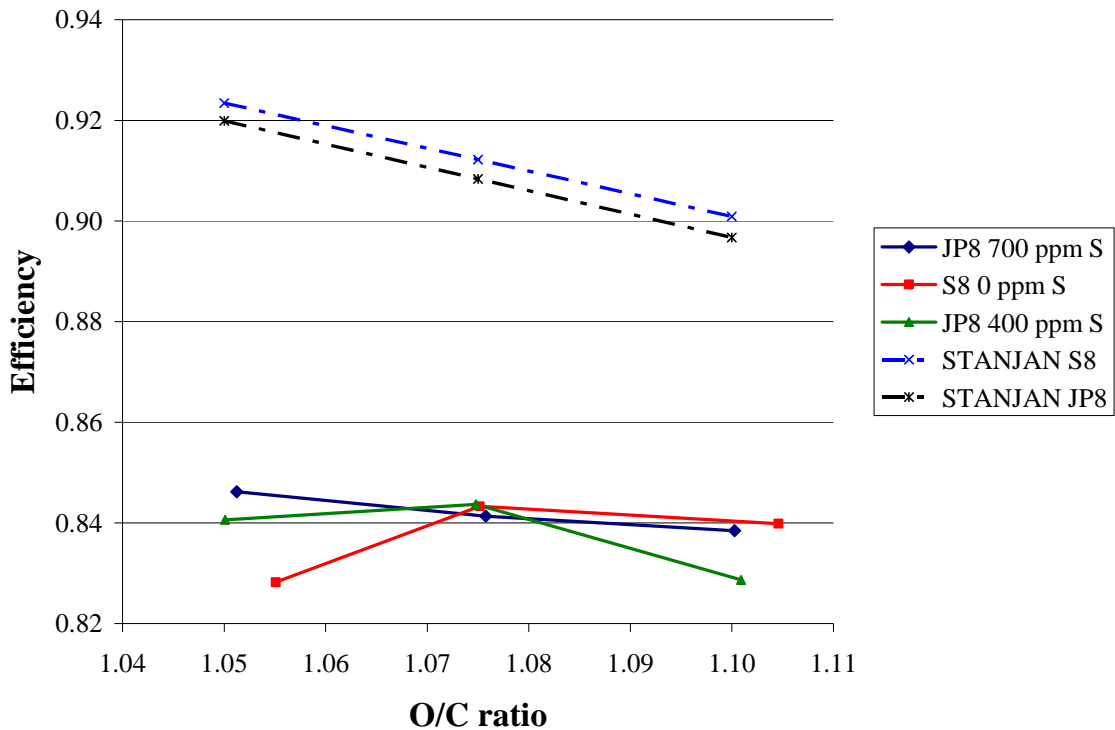


Figure 28: Efficiency of Aspen Reformer with various fuels and modeled fuels with respect to O/C ratios

From Figure 28, JP8 with 700 ppm S has the highest efficiency (84.62%) at an O/C ratio of 1.05. JP8 with 400 ppm S has the highest efficiency (84.37%) at an O/C ratio of 1.075. S8 has the highest efficiency (84.37%) at an O/C ratio of 1.075. S8 had lower CPOX temperatures than JP8 by 15°C to 20°C. The lower CPOX temperatures are attributed to aromatics having a higher heat of reaction. The aromatic fuels could be performing better due to the desulfurization beds cracking the fuel and oxygenating the fuel making the conversion to CO and hydrogen easier. To help project the efficiency of each fuel at the design point, linear trend lines were added to all the plots for the reformate components in terms of mole fraction. The equations of the lines were used to

calculate mole fractions at varying O/C ratios. With the new values of mole fractions for CO, CO₂, H₂, and N₂, the efficiency of the system was calculated. The values for temperature were also projected out to ensure the system remained higher than 950°C and less than 1100°C to make sure coking would not occur and the catalyst would not be damaged from the heat.

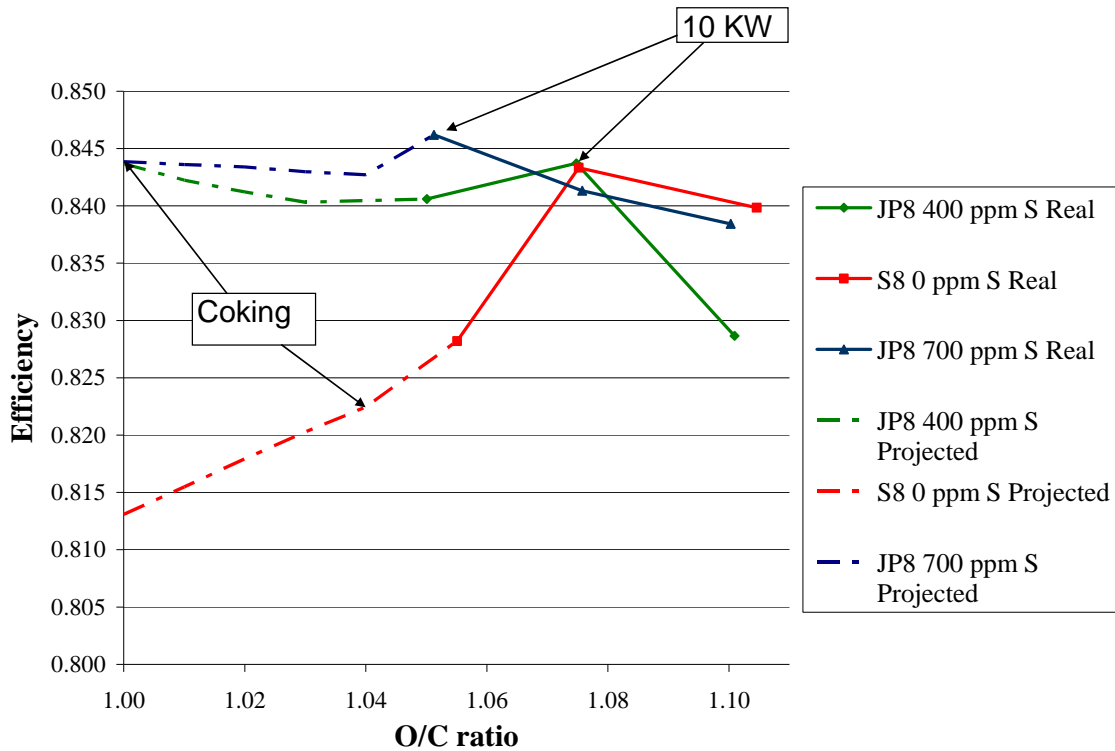


Figure 29: Projected efficiency values for the Aspen reformer with varying O/C ratios for various fuels

Figure 29 shows the projected efficiency and actual data from the Aspen reformer for varying O/C ratios. The highest efficiency of the system for S8 and JP8 with 400 ppm S is at an O/C ratio of 1.075. At this point these fuels reach 10 kW of thermal energy, the maximum energy for this system. JP8 with 700 ppm reached the highest efficiency at

1.05 and produced 10 kW of thermal energy at this point. S8 is projected to produce coking at an O/C ratio of 1.04 and JP8 with 700 ppm S will produce coking at 1.00. S8 is projected to continue to decrease in efficiency as the O/C ratio decreases. The projected data for JP8 with 700 ppm sulfur initial decrease in efficiency from an O/C of 1.05 to 1.04. Then the projected data shows a small increase in efficiency by decrease the O/C ratio from 1.04 to 1.00 of 0.0012%. JP8 with 400 ppm S shows a similar trend and the efficiency decrease from an O/C ratio 1.04 to 1.05. The trend then begins to increase from an O/C ratio of 1.04 to 1.00 by 0.0024%. Table 5 has the design points from the Aspen reformer to aid in the understanding of how the O/C ratios affect the reformat compositions.

Table 5: Design points for Aspen reformer with varying fuels

		O/C ratios	
	JP8 400	S8	JP8 700
Maximize H2	1.05	1.075	1.075
Maximize CO	1.075	1.05	1.05
Minimize CO2	1.075	1.075	1.075
Maximize Efficiency	1.075	1.075	1.05

V. Conclusions and Recommendations

Conclusions of Research

S8 is a viable fuel to use in fuel reforming to provide reformat for fuel cells. While S8 did not achieve the same efficiency as JP8 with 700 ppm of S in testing it proved to be comparable to JP8 with 400 ppm S. The aromatic fuels could be performing better due to the desulfurization beds cracking the fuel and oxygenating the fuel making the conversion to CO and hydrogen easier. The encouraging factor with S8 is since it is a sulfur free fuel, the desulfurization beds could be removed from the Aspen fuel reformer causing a decrease in weight and an increase in the power density. The current power density of the unit is 125 W/kg and by removing the desulfurization beds the power density would increase to 130.1 W/kg. By removing the desulfurization beds from the system the start up time could be reduced by 2 to 2 ½ hours. S8 has fewer aromatics than the JP8 fuels; this helps reduce any coking issues arising when runs are attempted with JP8 at lower O/C ratios and lower temperatures. S8 has a higher heat of combustion value 44.11 MJ/kg, versus JP8 with a heat of combustion of 43.32 MJ/kg. With more energy going into the system, it would therefore be possible to get more energy out with the same efficiency.

Stanjan modeling has proven to be a useful tool to use with the results from these tests on the reformer. Stanjan showed trends and helped predict how S8 would differ from JP8. While Stanjan can only provide equilibrium calculations, it offers values useful to measure against to see how close the reformer gets to equilibrium. Stanjan calculations are also useful in determining the design point of the reformer. The

calculations showed the reformer should be operated around an O/C ratio of 1.0 to 1.03. The projected value for JP8 agreed with the Stanjan modeling, operating around an O/C of 1.0 would provide the best efficiency.

Significance of Research

This is of interest since these fuels are readily available for military applications and can be used to provide reformat to the fuel cells needed to power auxiliary devices, a viable remote power source. The research provides vital information on long chain hydrocarbon fuels not well studied with catalytic partial oxidation. Previous studies to investigate hydrocarbon fuels in catalytic partial oxidation did not provide information on S8 and JP8. S8 in comparison with JP8 is important to determine if S8 would be an alternative fuel to use in reforming.

Recommendations for Future Research

Additional testing of the fuels needs to be performed over a wider range of O/C ratios. Through examination of various O/C ratios for each fuel, the design point and maximum efficiency could be enhanced. Running tests over the projected O/C range would give a more complete set of data. Since the reformer is designed with desulfurization beds there were some thoughts that S8 might not operate well in the system. This reforming system was designed for fuel with aromatics and sulfur content, and the high pressure and temperature in the desulfurization beds will cause a breaking of the bonds for the aromatics to get rid of the sulfur. The sulfur then is joined with oxygen or hydrogen and sent to the fuel tank to be vented out. One potential explanation could be the more aromatic fuel could be performing better because the desulfurization beds oxygenate the

fuel and make for easier conversion to reformat. With future runs the amount of energy into the system should be held constant instead of the amount of fuel into the system. Making these values equal will make the energy out of the system calculations more meaningful to see if S8 does outperform JP8.

The main problem with fuel reforming is dealing with the sulfur and coking issues. The Aspen reformer successfully addressed the sulfur issue by including desulfurization beds. This success was seen in Figure 23, which shows there is no decrease in hydrogen production over a period of time.

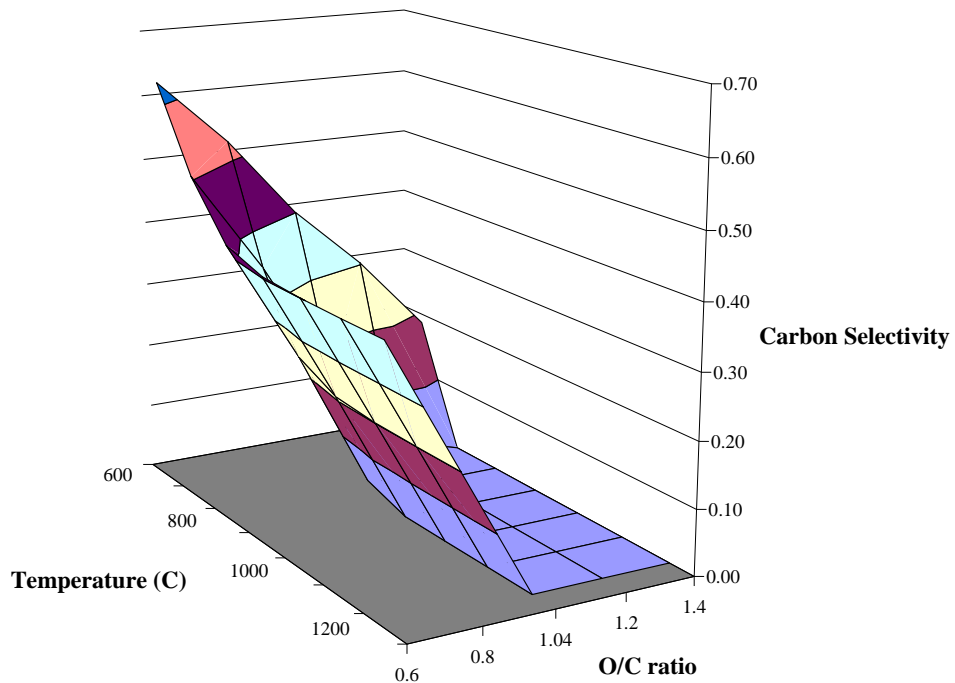


Figure 30: CPOX reforming of JP8 with varying O/C ratios with respect to temperature

Figure 30 using Stanjan shows coking can be avoided only at high temperatures and high O/C ratios. By increasing the O/C ratios above 1.0, hydrogen and carbon monoxide will

decrease, which are desired products in the reformat. Steam reforming can address the issue of coking when the steam to carbon ratio is over one.

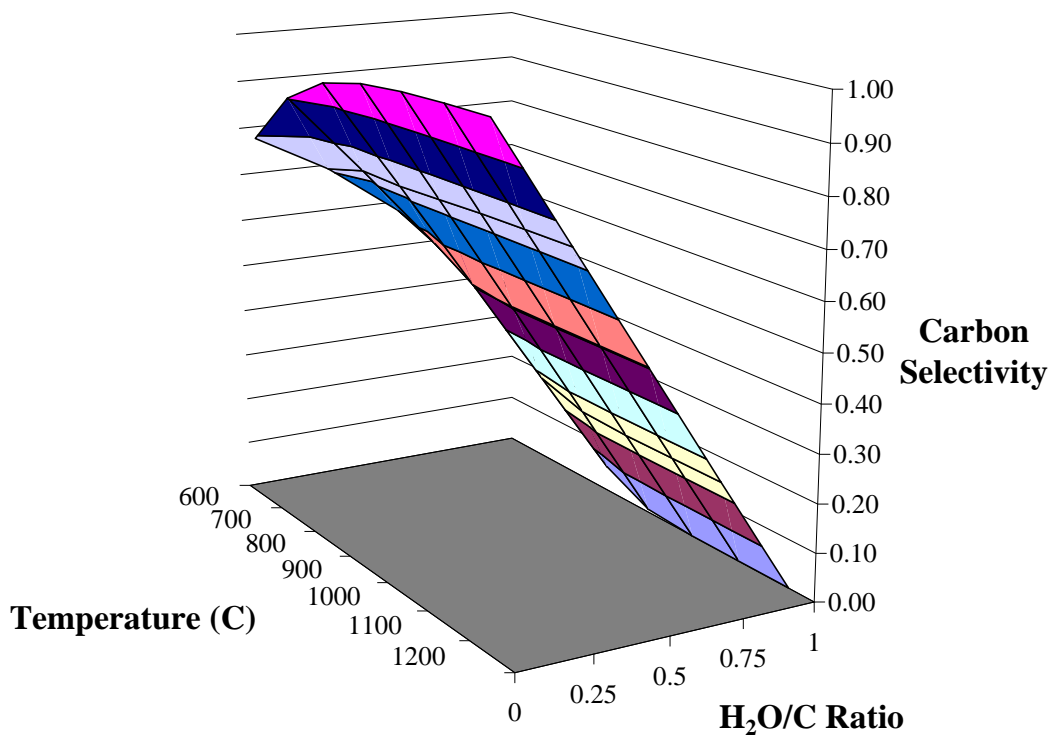


Figure 31: Steam reforming of JP8 with varying steam to carbon ratios with respect to temperature

The drawback of steam reforming is energy must continually be put into the system to provide the heat to produce steam. This heat could be provided from the rejected heat from SOFC or MCFC. Steam reforming is of interest due to it having the highest efficiency of all fuel reforming. With the CPOX process being exothermic, this energy could ideally be used with steam reforming to produce steam.

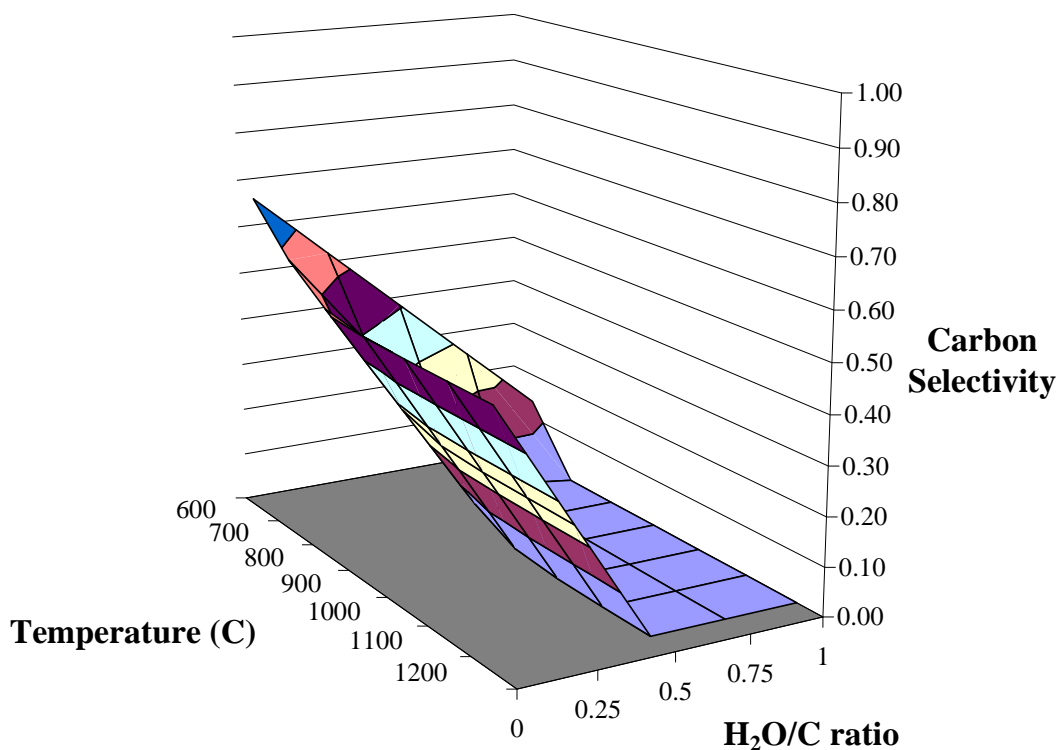


Figure 32: Auto-thermal reforming with JP8 varying steam to carbon ratios with respect to temperature

The issue with coking can be addressed with auto-thermal reforming without having high O/C or steam to carbon ratios. For future research steam reforming of JP8 and S8 will be investigated. This research will begin with smaller hydrocarbon fuels such as propane and the larger hydrocarbon fuels will be used to see if the results can be predicted with reaction rates. The quartz reactor in this experiment will have an 8 mm inner diameter so approximately 0.1 grams of catalyst will be used. The catalyst used in this study will be a Pd/alumina and Rh/alumina. The total gas flow of the system will be between 100 to 120 ml/min to give a space velocity of 66,000 ml/(g*hr).

Appendix

Table 6: Sample calculation for GC data on JP8 with 700 ppm

sulfur

Ret Time	Width	Area	Column	TRF	Rel Response	Mole Rel to N2		Mole Fraction
1.503	0.293	9871	Q	39.4	250.533			
		4958.7	Q	42	118.065			
		4912.3	Q	42	116.959			
1.847	0.267	40	Q	48	0.833	0.0127	CO2	0.0065
2.403	0.95	12484	MS	420	29.724	0.4518	H2	0.2303
4.803	0.987	2763	MS	42	65.786		N2	0.5096
9.62	1.807	1375	MS	42	32.738	0.4976	CO	0.2536

The thermal response values (TRF) were taken from Dietz 1967.

Table 7: Sample calculation for mass balance on JP8 with 700 ppm sulfur

Air Flow (SLPM)	72.2	Mol C/min	1.1743	Mol H/min	2.2589
Fuel Flow (cc/m)	21	Mol O/min	1.2343	Mol N2/min	2.3031
Temp (C)	984	O/C Ratio	1.0511	Total Moles	4.5191
C grams/min	14.1032	H grams/min	2.2768		
O grams/min	19.7473	N2/grams min	64.5190		
		Total grams in	100.6463		
	Moles (out)	Mass out (grams)		Mass balance	
CO2	0.0292	1.2840		0.9935	
H2	1.0406	2.0979			
N2	2.3031	64.5112			
CO	1.1462	32.1038			
	Total grams out	99.9970			

Table 8: Sample calculations for Efficiency and Power on JP8 with 700 ppm sulfur

Efficiency	Power Output MJ/min	Power Input MJ/min
0.8763	0.6218	0.7096
	Power Out kW	Power Input kW
	10.363	11.827

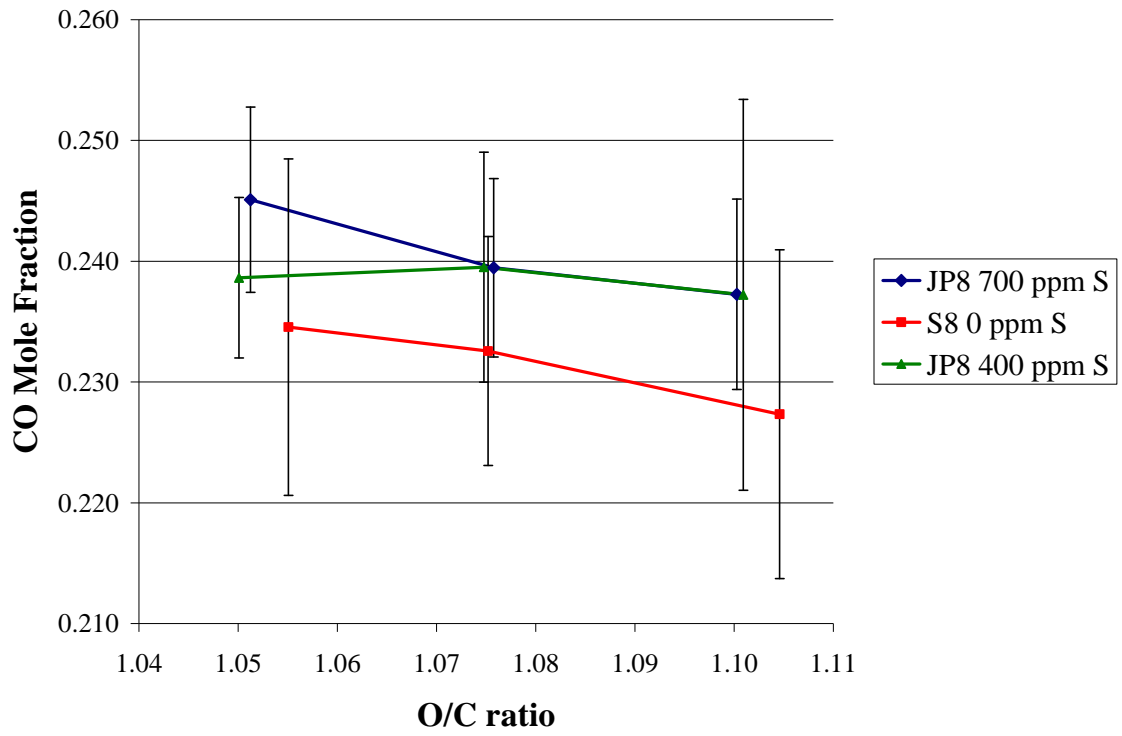


Figure 33: CO varying O/C ratio with statistical error

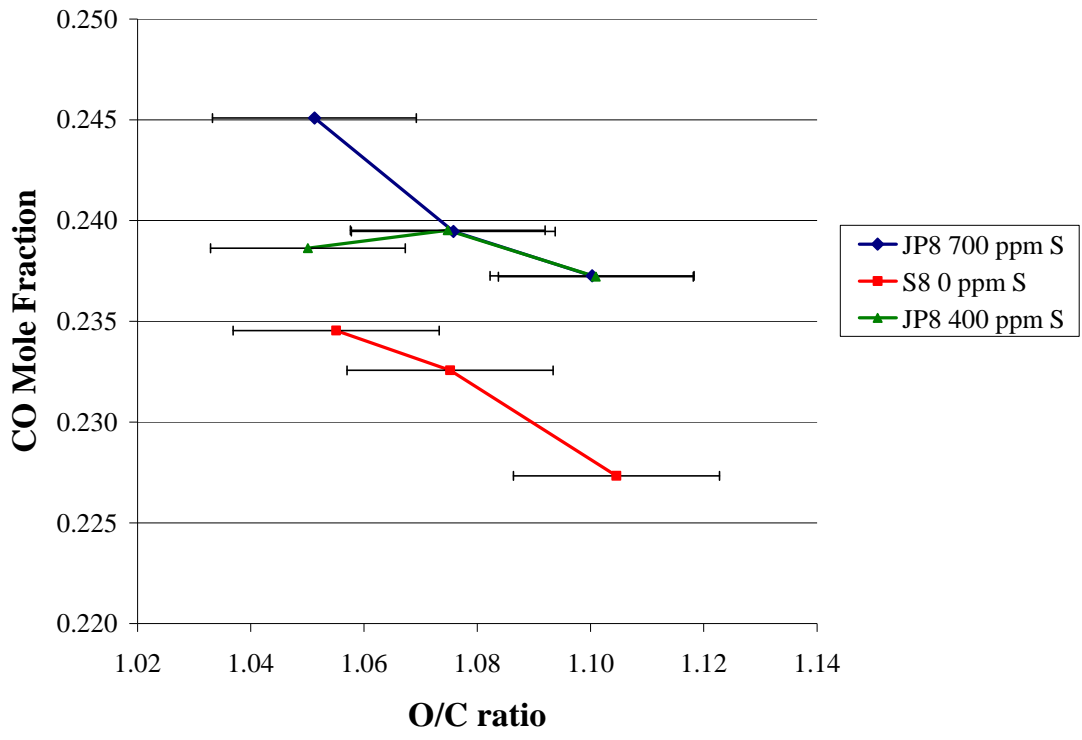


Figure 34: CO varying O/C ratios showing O/C ratio systematic error

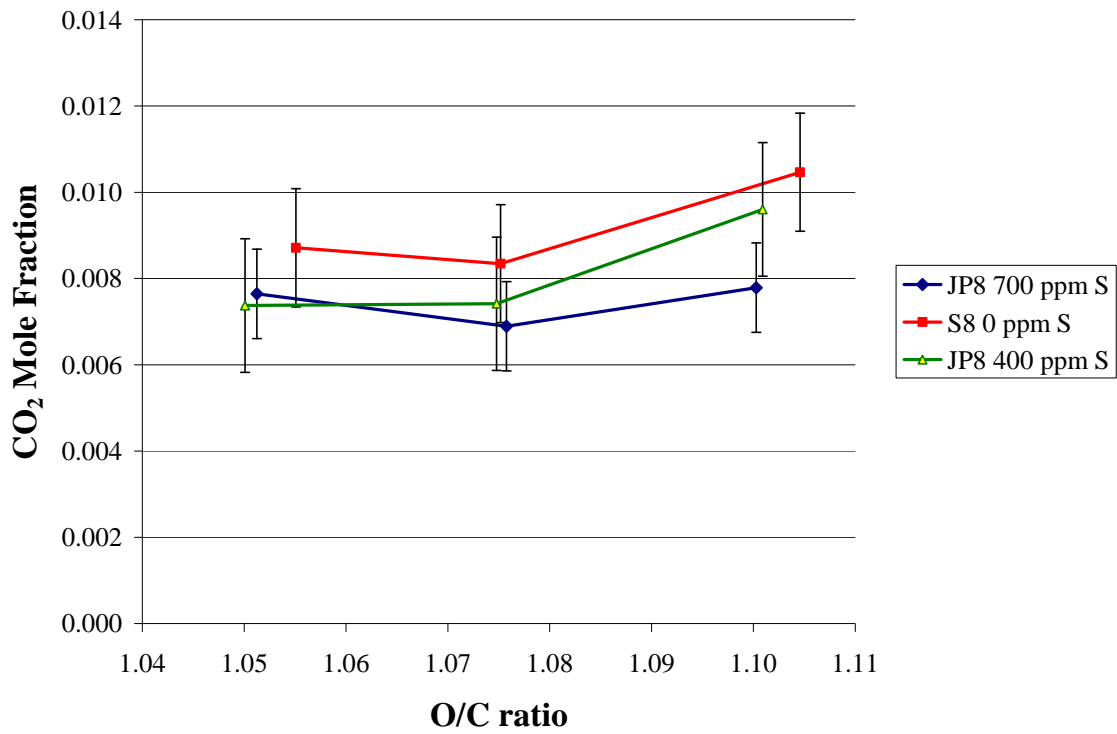


Figure 35: CO₂ varying O/C ratios with statistical error

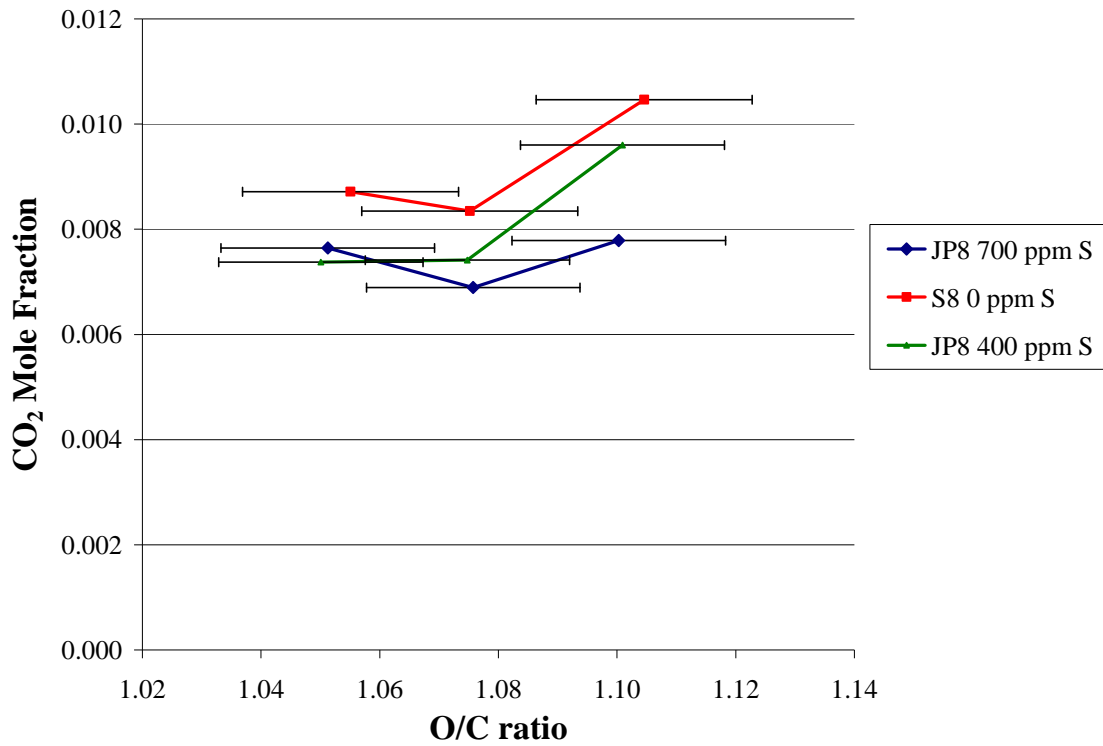


Figure 36: CO₂ varying O/C ratios showing O/C ratio systematic error

Bibliography

1. Burcat, Alexander *Ideal Gas Thermodynamic Data in Polynomial form for Combustion and Air Pollution Use*. 9 May 2007
<http://garfield.chem.elte.hu/Burcat/burcat.html>
2. Campbell, Timothy J., Aly H. Shaaban, Franklin H. Holcomb, Reza Salavani, and Michael J. Binder. "JP-8 catalytic cracking for compact fuel processors," *Journal of Power Sources*, 129: 81-89 (15 April 2004).
3. Cheekatamarla, Praveen K. and Alan M. Lane. "Catalytic autothermal reforming of diesel fuel for hydrogen generation in fuel cells: I. Activity test and sulfur poisoning," *Journal of Power Sources*, 152: 256-263 (1 December 2005).
4. Corbo, Pasquale and Fortunato Migliardini. "Hydrogen production by catalytic partial oxidation of methane and propane on Ni and Pt catalyst," *International Journal of Hydrogen Energy*, in press (24 July 2006).
5. Dietz, W.A. "Response factors for gas chromatographic analyses," *Journal of Gas Chromatography*, 5: 68-71 (1967).
6. Dreyer, B.J., I.C. Lee, J.J. Krummenacher, and L.D. Schmidt. "Autothermal steam reforming of higher hydrocarbons n-Decane, n-hexadecane and JP-8," *Applied Catalysis A: General*, 307: 184-194 (3 July 2006).
7. Edwards, Tim. "'Kerosene' Fuels for Aerospace Propulsion- Composition and Properties," *38th AIAA/ASME/SAE/ASEE Joint Propulsion Conference & Exhibit*. AIAA Paper 2002-3874. Indianapolis, Indiana: July 7-10, 2002.
8. Gardner, Todd H., David A. Berry, K. David Lyons, Stephen K. Beer, and Adam D. Freed. "Fuel processor integrated H₂S catalytic partial oxidation technology for sulfur removal in fuel cell power plants," *Fuel*, 81: 2157-2166 (December 2002).
9. Hardiman, Kelfin M., Tan T. Ying, Adesoji A. Adesina, Eric M. Kennedy, and Bogdan Z. Dlugogorski. "Performance of Co-Ni catalyst for propane reforming under low steam-to-carbon ratios," *Chemical Engineering Journal*, 102: 119-130 (September 2004).
10. Krummenacher, Jakob J., Kevin N. West, and Lanny D. Schmidt. "Catalytic partial oxidation of higher hydrocarbons at millisecond contact times: decane, hexadecane, and diesel fuel," *Journal of Catalysis*, 215: 332-343 (25 April 2003).
11. Larminie, James and Andrew Dicks. *Fuel Cell Systems Explained*. New York: Wiley, 2000.

12. Lenz, Bettina and Thomas Aicher. "Catalytic autothermal reforming of Jet fuel," *Journal of Power Sources*, 149: 44-52 (26 September 2005).
13. Lutz, Andrew E., Robert W. Bradshaw, Leslie Bromberg, and Alex Rabinovich. "Thermodynamic analysis of hydrogen production by partial oxidation reforming," *International Journal of Hydrogen Energy*, 29: 809-816 (July 2004).
14. Montgomery C. J., S. M. Cannon, M.A. Mawid, and B. Sekar. "Reduced Chemical Kinetic Mechanisms for JP-8 Combustion," *40th AIAA Aerospace Science Meeting and Exhibit*. AIAA Paper 2002-0336. Reno, Nevada: Jan. 14-17, 2002.
15. Moon, Dong J., Jong Woo Ryu, Sang Deuk Lee, Byung Gwon Lee, and Byoung Sung Ahn. "Ni-based catalyst for partial oxidation reforming of iso-octane," *Applied Catalyst A: General*, 272: 53-60 (28 September 2004).
16. Paulus, U.A., U. Endruschat, G.J. Feldmeyer, T.J. Schmidt, H. Bonneman, and R.J. Behm. "New PtRu alloy colloids as precursors for fuel cell catalyst," *Journal of Catalysis*, 195: 383-393 (25 October 2000).
17. Perry, Robert H., and Cecil H. Cliton. *Chemical Engineers' Handbook*. New York: McGraw Hill, 1973.
18. Phaharso, A.A. Adesina, D.L. Trimm, and N.W. Cant. "Kinetic study of iso-octane steam reforming over a nickel-based catalyst," *Chemical Engineering Journal*, 99: 131-136 (15 June 2004).
19. W. C. Reynolds, *Stanjan: interactive computer programs for Chemkin equilibrium analysis*. Stanford University Report, January 1986.
20. Shekhawat, Dushyant, Todd H. Gardner, David A. Berry, Maria Salazar, Daniel J. Haynes, and James J. Spivey. "Catalytic partial oxidation of n-tetradecane in the presence of sulfur of polynuclear aromatics: Effects of support on metal," *Applied Catalysis A: General*, 311: 8-16 (September 2006).
21. Song, Chunshan. "Fuel Processing for low-temperature and high temperature fuel cells: Challenges, and opportunities for sustainable development in the 21st century," *Catalysis Today*, 77: 17-49 (December 2002).
22. United States Department of Energy. *Hydrogen, Fuel Cells & Infrastructure Technologies Program*. 9 May 2007
http://www1.eere.energy.gov/hydrogenandfuelcells/fuelcells/fc_types.html
23. Wang, Linsheng, Kazuhisa Murata, and Megumu Inaba. "Steam reforming of gasoline promoted by partial oxidation reaction on novel bimetallic Ni-based

catalysts to generate hydrogen for fuel cell powered automobile applications,”
Journal of Power Sources, 145: 707-711 (18 August 2005).

24. Wang, X. and R.J. Gorte. “A study of steam reforming of hydrocarbon fuels on Pd/ceria,” *Applied Catalysis A: General*, 224: 209-218 (25 January 2002).

Vita

Thomas G. Howell graduated from Wayne High School in Huber Heights, Ohio in 2000. He then continued his education at Wright State University in Dayton, Ohio. He graduated from Wright State University in June of 2005 with a Bachelor of Science in biomedical engineering. He received a Dayton Area Graduate School Institute scholarship to work on his Master's at the Air Force Institute of Technology. Once he completes his Master's at AFIT, he will continue working for UES Inc and pursue a PhD in material science at the University of Cincinnati.

REPORT DOCUMENTATION PAGE				<i>Form Approved OMB No. 074-0188</i>	
<p>The public reporting burden for this collection of information is estimated to average 1 hour per response, including the time for reviewing instructions, searching existing data sources, gathering and maintaining the data needed, and completing and reviewing the collection of information. Send comments regarding this burden estimate or any other aspect of the collection of information, including suggestions for reducing this burden to Department of Defense, Washington Headquarters Services, Directorate for Information Operations and Reports (0704-0188), 1215 Jefferson Davis Highway, Suite 1204, Arlington, VA 22202-4302. Respondents should be aware that notwithstanding any other provision of law, no person shall be subject to a penalty for failing to comply with a collection of information if it does not display a currently valid OMB control number. PLEASE DO NOT RETURN YOUR FORM TO THE ABOVE ADDRESS.</p>					
1. REPORT DATE (DD-MM-YYYY) 14-June-2007		2. REPORT TYPE Master's Thesis		3. DATES COVERED (From - To) September 2006 - June 2007	
4. TITLE AND SUBTITLE CATALYTIC PARTIAL OXIDATION REFORMING OF JP8 AND S8				5a. CONTRACT NUMBER	
				5b. GRANT NUMBER	
				5c. PROGRAM ELEMENT NUMBER	
6. AUTHOR(S) Howell, Thomas G.				5d. PROJECT NUMBER	
				5e. TASK NUMBER	
				5f. WORK UNIT NUMBER	
7. PERFORMING ORGANIZATION NAMES(S) AND ADDRESS(S) Air Force Institute of Technology Graduate School of Engineering and Management (AFIT/EN) 2950 Hobson Way, Building 640 WPAFB OH 45433-8865				8. PERFORMING ORGANIZATION REPORT NUMBER AFIT/GAE/ENY/07-J08	
9. SPONSORING/MONITORING AGENCY NAME(S) AND ADDRESS(ES) Dr. Thomas Reitz AFRL/PRPS 1950 Fifth Street, Building 18G WPAFB OH 45433-7765				10. SPONSOR/MONITOR'S ACRONYM(S)	
				11. SPONSOR/MONITOR'S REPORT NUMBER(S)	
12. DISTRIBUTION/AVAILABILITY STATEMENT APPROVED FOR PUBLIC RELEASE; DISTRIBUTION UNLIMITED					
13. SUPPLEMENTARY NOTES					
14. ABSTRACT Catalytic partial oxidation (CPOX) reforming experiments were performed using a 10 kW Aspen Products Group, Inc. fuel processing prototype utilizing military logistic fuels JP8 and S8. S8 is a sulfur-free Fisher-Tropsch fuel, while JP8 is a multi-fuel blend, which could impact reforming efficiency, product distribution and byproduct production. Sulfur contained within the JP8 will adversely affect the product distribution; therefore, desulfurization beds, capable of removing up to 1000 ppm sulfur, were incorporated into the system. The catalyst used in the prototype is noble metal dispersed on cordierite monolith. The goal of this experiment was to evaluate the efficiency and product distribution of the prototype fuel processor through application of several potential military fuels. These results are compared with computational models (Stanjan) to determine if CPOX reactions can be appropriately modeled. JP8 with 700 ppm of sulfur had the highest efficiency of 84.62% followed by JP8 with 400 ppm of sulfur at 84.37% and S8 at 84.37%.					
15. SUBJECT TERMS Catalytic partial oxidation, S8, JP8, sulfur, coking, steam reforming, autothermal reforming					
16. SECURITY CLASSIFICATION OF:			17. LIMITATION OF ABSTRACT UU	18. NUMBER OF PAGES 82	19a. NAME OF RESPONSIBLE PERSON Richard Branam, Major, USAF
a. REPO RT U	b. ABSTRA CT U	c. THIS PAGE U			19b. TELEPHONE NUMBER (Include area code) (937) 255-6565, ext 7485 (Richard.branam@afit.edu)

